REPRINT AND ACCEPTED MANUSCRIPT

Phatchaneeya Thammawong · Watchara Kasinrerk · Raymond J. Turner · Chatchai Tayapiwatana

Twin-arginine signal peptide attributes effective display of CD147 to filamentous phage

Received: 12 August 2005 / Revised: 26 October 2005 / Accepted: 1 November 2005 / Published online: 1 December 2005 © Springer-Verlag 2005

Abstract A novel phagemid (pTat8) was constructed in this study to improve the quality of a molecule displayed on filamentous phage. The twin-arginine translocation (Tat) pathway was chosen for transporting and integrating a CD147 molecule into a phage particle via gpVIII. The parent vector pComb8-CD147Ex was modified by substituting a Sec signal sequence (PelB) with a twin-arginine signal sequence from trimethylamine N-oxide reductase (TorA). The characteristics of the CD147 displayed on the phage particle were evaluated by Sandwich ELISA and Western immunoblotting. A Tat-dependent leader was found to be superior to the Sec leader for the phage display of CD147. Our findings further support the involvement of an Escherichia coli Tat translocase in mediating the integration of a hydrophobic transmembrane protein into the inner membrane. This modified phagemid will be useful in phage display technique when the correctly folded structure is required (i.e., antibody libraries and ligand-receptor tracing).

This work was supported by the Thailand Research Fund and the National Center for Genetic Engineering and Biotechnology, R.J.T. thanks the Canadian Institutes of Health Research for funding support.

P. Thammawong · W. Kasinrerk · C. Tayapiwatana (☒) Division of Clinical Immunology, Department of Medical Technology, Faculty of Associated Medical Sciences

Chiang Mai University, Chiang Mai 50200, Thailand e-mail: asimi002@hotmail.com

Tel.: +66-53-945080 Fax: +66-53-946024

W. Kasinrerk

Medical Biotechnology Unit, The National Center for Genetic Engineering and Biotechnology, National Science and Technology Development Agency, Faculty of Associated Medical Sciences, Chiang Mai University, Chiang Mai 50200, Thailand

R. J. Turner Department of Biological Sciences, University of Calgary, 2500 University Drive NW, T2N 1N4 Calgary Alberta, Canada

Introduction

Phage display is a powerful technique for engineering proteins or peptides. In this technique, a bacteriophage is used as a vehicle to express diverse polypeptides as part of a phage coat protein (i.e., gpIII or gpVIII). The strategy for expressing the fusion protein is to insert the DNA-coding fragment of interest between the signal sequence and the phage coat protein genes. Upon viral infection, recombinant proteins, together with other coat proteins, are synthesized in the bacterial host and directly translocated to the inner membrane, where a signal peptide is cleaved before incorporation into the phage progeny (Barbas et al. 2001).

The general secretory (Sec) pathway is a general bacterial protein translocation system (Pugsley 1993). The proteins exported via Sec machinery are synthesized with an N-terminal signal peptide that directs translocation in an unfolded state by an apparatus consisting of soluble and membrane-bound Sec gene products (Danese and Silhavy 1998). The phagemids that are applied in phage display technique usually contain Sec signal sequences such as OmpA and OmpT (Manosroi et al. 2001; Heyd et al. 2003).

The translocation rate of proteins delivered through the Sec pathway is quite rapid, at about 10,000 amino acids per minute (Vallejo and Rinas 2004). However, the folding rate of some heterologously expressed chimeric proteins can be very fast compared to the translocation that results in an incompatible substrate for the Sec channel. Consequently, unfolded proteins, which have not yet buried their hydrophobic amino acid stretches or have had the chance to pass through the Sec channel, tend to form inclusion bodies in the periplasmic space (Mitraki et al. 1991; Vallejo and Rinas 2004). Taken together, an efficient protein secretion pathway is required for displaying an active protein on a phage particle.

In recent years, it has become clear that most bacteria possess a second general protein translocation pathway that is quite distinct from the Sec apparatus. This Sec-independent pathway has been termed the twin-arginine translo-

cation (Tat) system (Berks 1996; Sargent et al. 1998). A signal peptide contains a peculiar motif, including two consecutive arginine residues (Santini et al. 1998). The most remarkable characteristic of the Tat pathway is that it functions in transporting folded proteins of varying dimensions across the cytoplasmic membrane (Berks et al. 2000). This pathway exports proteins in their native conformation, since the folding process occurs before translocation, thus enabling cytoplasmic chaperones and foldases to be used, reducing the amount of aggregation either in the cytoplasm or in the periplasm.

In this study, the Tat system was used to improve the quality of the displayed molecule CD147 on the phage particle. CD147 is a human leukocyte surface molecule of the immunoglobulin superfamily and is found on the surface of various cell types (i.e., cancer cells and activated T lymphocytes) (Kasimrerk et al. 1992, 1999; Biswas et al. 1995). A suitable method to produce functional CD147 is needed for the study of molecular and cellular CD147 functions.

Materials and methods

Site-directed mutagenesis of pComb8-CD147Ex phagemid

Site-directed mutagenesis was applied to make an NsiI restriction site upstream of the PelB signal sequence in the pComb8-CD147Ex phagemid (Intasai et al. 2003) by using primers MutPelBa (5'-GAG ACA GTC ATA atg cat TAC CTA TTG CCT ACG-3') and MutPelBb (5'-CGT AGG CAA TAG GTA atg cat TAT GAC TGT CTC-3') (the NsiI restriction site is designated by lower-case letters). Polymerase chain reaction (PCR) was carried out using PfuTurbo DNA polymerase (Stratagene, La Jolla, CA, USA) according to the QuikChange Site-Directed Mutagenesis Kit protocol. Subsequently, the mixture was treated with DpnI (Promega, Madison, WI, USA) to digest the nonmutated parental vector. The resulting phagemid was named MpComb8-CD147Ex. MpComb8-CD147Ex was digested with NsiI and XbaI (Fermentas, Massachusetts, USA) to prepare the cloning site. After purification, the 5'end was dephosphorylated to prevent the recircularization and religation of linear-digested MpComb8-CD147Ex, using calf intestinal alkaline phosphatase (Promega).

TorA signal sequence amplification by PCR

Two oligonucleotides—TatNsiIFw (5'-GAG GAG GAG GTa tgc atA ATA ACG ATC TCT TTC AG-3') with an NsiI restriction site (lower-case letters) and TatXhoIRev (5'-GAG GAG GAG CTc tcg agC GCC GCT TGC GCC GCA GT-3') with an XhoI restriction site (lower-case letters)—were used as primers for amplifying the TorA signal sequence gene from the pSPL04 vector (kindly

provided by Dr. J.H. Weiner, University of Alberta, Canada) using ProofStart DNA polymerase. After amplification cycles, the resulting 126-bp PCR product was analyzed by gel electrophoresis, subsequently treated with *NsiI* and *XhoI* (Fermentas), and purified with a QIAquick PCR purification kit (Qiagen).

Construction of phagemid containing *Tat-CD147Ex* gene

The pComb8-CD147Ex phagemid was digested with Xhol and Xbal. The DNA fragment of digested pComb8-CD147Ex containing the CD147 gene of 844 bp was subsequently ligated with a digested TorA signal sequence PCR product, using T4 ligase enzyme (Roche Molecular Biochemicals, Mannheim, Germany). The 970-bp ligation product was named Tat-CD147 fragment. The Tat-CD147 ligated product was further amplified using primers TatNsiIFW and Tat-CD147Rv (5'-GAG GAG GAG CTt cta gaA CTG ACG AGC TC-3'; the Xbal restriction site is designated by lower-case letters). After purification, the PCR product was digested with Nsil and Xbal.

The *Nsi*I- and *Xba*I-digested Tat-CD147 fragment was ligated with the dephosphorylated *Nsi*I- and *Xba*I-digested MpComb8-CD147Ex by the T4 ligase enzyme (Fermentas). The newly constructed phagemid was named pTat8-CD147. The phagemid was transformed into TG-1 wild type and Δ*tatABC* mutant strain (DSS640) (a gift from Dr. J.H. Weiner, University of Alberta) (Sambasivarao et al. 2001). Transformed cells were selected on Luria–Bertani agar containing 100 μg/ml ampicillin.

Phage display of CD147Ex via gpVIII

After transforming TG-1 with pTat8-CD147, the phage display technique was performed using the phage display of CD147 through the Sec pathway protocol, as described previously (Intasai et al. 2003). Briefly, a clone of pTat8-CD147-transformed TG-1 was grown in 10 ml of 2× tryptone-yeast (TY) broth [1.6% (wt/vol) tryptone, 1% (wt/vol) yeast extract, and 0.5% (wt/vol) sodium chloride] containing 100 µg/ml ampicillin at 37°C until an optical density (OD) at 600 nm of 0.8 was reached. Precultured bacteria were subsequently propagated in 100 ml of the same medium containing 2 ml of 50% glucose and then cultured at 25°C until 0.5 OD. Then 30 ml of the culture was infected with VCSM13 helper phage. The phageinfected TG-1 was spun down at 3,000 rpm for 10 min at 4°C. The pellet was resuspended in 30 ml of 2× TY broth containing ampicillin (100 µg/ml) and kanamycin (70 µg/ ml) and then transferred to 220 ml of the same broth and shaken at 180 rpm for 16 h at 25°C. Bacteriophages harboring CD147Ex via gpVIII generated by the Tat pathway (ΦTat-CD147gpVIII) were harvested by PEG 8000/NaCl precipitation (Tayapiwatana and Kasinrerk

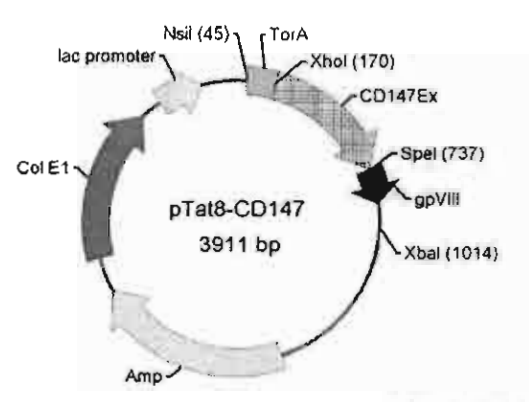


Fig. 1 Map of the pTat8-CD147 phagemid. The Nsil- and Xbalcloning sites are areas where the Tat-CD147 fragment was inserted. The origin of replication (Col E1), lac promoter, Tat signal sequence (TorA), and gpVIII are shown

2002). Finally, the phages were reconstituted with 2.5 ml of 0.15 M phosphate-buffered saline (PBS), pH 7.2, and centrifuged at 11,000 rpm for 10 min at 4°C.

Immunoassay for phage-displayed CD147ExgpVIII by Sandwich ELISA

A microtiter plate (NUNC, Roskilde, Denmark) was coated with 50 μl of 10 μg/ml CD147 monoclonal antibodies (mAb) (M6-1E9, IgG_{2a}; M6-1D4, IgM; M6-1F3, IgM; M6-2B1, IgM; M6-2F9, IgM) (Kasinterk et al. 1999) in a carbonate/bicarbonate buffer, pH 9.6. Two of five mAb (M6-1E9 and M6-1D4) recognize linear epitopes of human CD147, while the other three mAb recognize conformational epitopes. Standard ELISA washing and blocking processes were performed. Recombinant phages were added to the wells

using the optimized phage amount (50 µl of 10¹⁰-10¹¹ cfu/ ml). Two alternative sets of anti-M13 mAb were used to monitor the binding of phage particles. One was horseradish peroxidase (HRP)-conjugated anti-gpVIII mAb (Amersham-Pharmacia Biotech, Buckinghamshire, UK). The other was biotinylated anti-gpIII mAb (Exalpha Biologicals, Massachusetts, USA). HRP-conjugated anti-biotin (Zymed, California, USA) was applied to trace biotinylated anti-gpIII mAb. After washing, the 3,3',5,5'-tetramethylbenzidine substrate was added and incubated at room temperature for color development. OD at 450 nm was determined after adding 1 N HCl to stop the reaction. Phage-displayed CD147Ex via gpVIII through the Sec pathway (\$\Phi\sec-CD147gpVIII), phagedisplayed CD147Ex via gpVIII prepared from the TG-1 ΔtatABC mutant strain (ΦTatmut-CD147gpVIII), and the VCSM13 helper phage were used to compare the absorbance unit obtained from ÖTat-CD147gpVIII by the ELISA system.

SDS-PAGE and Western immunoblotting

Protein components of precipitated phages were separated on a 12% polyacrylamide gel by sodium dodecyl sulfate—polyacrylamide gel electrophoresis (SDS-PAGE) in reducing conditions. For Western immunoblotting, the separated proteins were electroblotted onto a polyvinylidene fluoride (PVDF) membrane. The blotted membrane was blocked with 5% skim milk in PBS, pH 7.2, and then incubated with pooled CD147 mAb (M6-1E9 and M6-1D4 at 5 μg/ml each). After washing, HRP-conjugated rabbit—anti-mouse immunoglobulins (Zymed) were added to the membrane. Immunoreactive bands were then visualized using the chemiluminescent substrate detection system (Amersham-Pharmacia Biotech).

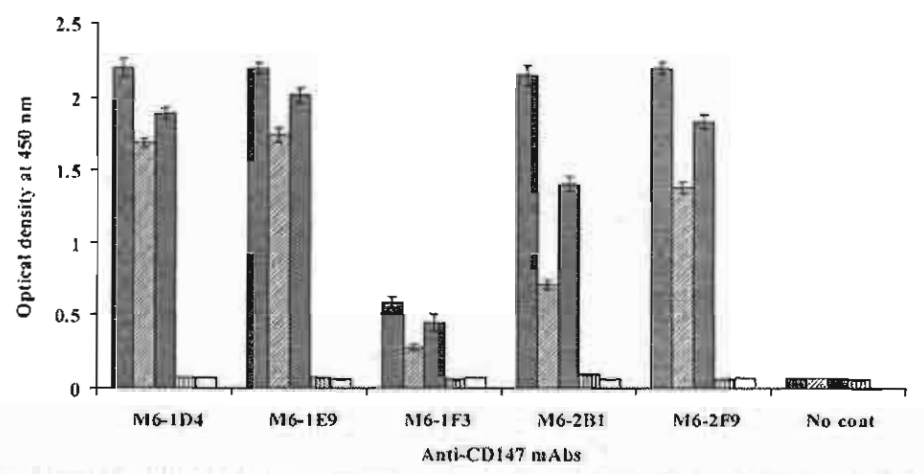
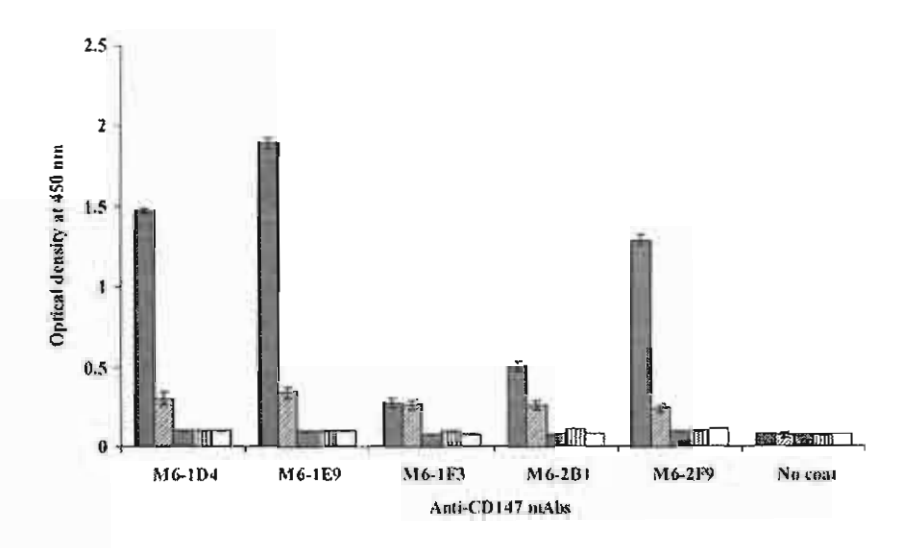


Fig. 2 Comparison of the expression of phage-displayed CD147Ex via the Tat and Sec pathways by Sandwich ELISA. Anti-CD147 mAb (M6-1D4, M6-1E9, M6-1F3, M6-2B1, and M6-2F9) were used to capture recombinant phages. The binding activity of each tested phage was compared using an arbitrary OD unit at 450 nm. This experiment was performed twice. Φ Tat-CD147gpVIII, phage-displayed CD147Ex on gpVIII via the Tat pathway (first bar);

ΦSec-CD147gpVIII, phage-displayed CD147Ex on gpVIII via the Sec pathway (second bar); ΦTatmut-CD147gpVIII, phage-displayed CD147Ex on gpVIII produced from the tat mutant (third bar); VCSM13 phage (forth bar); no phage (last bar). Phages were prepared from a culture supernatant by standard PEG/NaCl precipitation method

Fig. 3 Detection of CD147Ex presenting on phage particles through gpVIII by Sandwich ELISA. Recombinant phages were captured with five anti-CD147 mAb (M6-1D4, M6-1E9, M6-1F3, M6-2B1, and M6-2F9). The biotinylated antigpIII mAb/HRP-conjugated anti-biotin detection system was used for tracing antibody-bound phages. The experiment was performed twice. Bar designations are the same as those used in Fig. 2. Phages were prepared from a culture supernatant by standard PEG/NaCl precipitation method



Results

Construction of pTat8-CD147 phagemid

To generate the phage expressing a CD147 molecule via the Tat pathway, the pComb8-CD147Ex phagemid was modified by substituting the leader sequence from PelB with that from TorA. The correct nucleotide sequence of TorA-CD147Ex-gpVIII was determined according to the dideoxychain terminator procedure using BigDye Terminator v3.1 Cycle Sequencing Kit (PE Applied Biosystems, California, USA). The resulting map of the novel constructed phagemid pTat8-CD147 is shown in Fig. 1.

Comparison of phage-displayed CD147Ex expression by Sandwich ELISA

The phage-displayed CD147Ex, via gpVIII through the Tat pathway (ΦTat-CD147gpVIII), was produced by infecting the pTat8-CD147-transformed TG-1 with the VCSM13 helper phage. In addition, phage display of the CD147 fusion protein from the TG-1 \(\Delta tatABC\) mutant was performed to validate the TorA signal peptide directing the CD147 fusion protein via the Tat pathway. The expression of recombinant CD147Ex-gpVIII through the Tat pathway was determined by Sandwich ELISA in comparison with the Sec pathway. A panel of anti-CD147 mAb (M6-1D4, M6-1E9, M6-1F3, M6-2B1, and M6-2F9) was used as capture antibodies. By using the HRPconjugated anti-gpVIII, ÖTat-CD147gpVIII showed an absorbance unit higher than that of ΦSec-CD147gpVIII, with all anti-CD147 mAb (Fig. 2). However, the absorbance unit of Tatmut-CD147gpVIII, which bound to mAb-coated wells, was comparable to ФTat-CD147gpVIII. None of the CD147 mAb captured VCSM13, which assured assay specificity. In addition, nonspecific binding of phages was ruled out because the signal could not be detected in any uncoated well.

Demonstration of anchored CD147Ex on phage particles by Sandwich ELISA

To confirm that the CD147 molecule was linked to phage particles, the biotinylated anti-gpIII mAb/HRP-conjugated anti-biotin detection system was applied. As shown in Fig. 3, ΦTat-CD147gpVIII showed a binding activity with most anti-CD147 mAb (except for M6-1F3 wherein a similar signal was observed) higher than that of ΦSec-CD147gpVIII. ΦTatmut-CD147gpVIII and VCSM13 were not recognized by any anti-CD147 mAb, and this result was also obtained in uncoated wells.

Western immunoblotting

 Φ Tat-CD147gpVIII, Φ Sec-CD147gpVIII, and Φ Tatmut-CD147gpVIII (10^{10} cfu each) were fractionated by SDS-

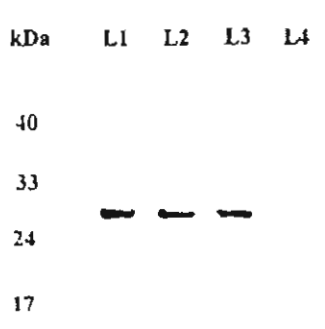


Fig. 4 Western immunoblotting of phage-displayed CD147Exgp-VIII. Phages were separated by SDS-PAGE in nonreducing conditions and transferred to a PVDF membrane. An immunological assay was performed by probing with a combination of anti-CD147 mAb (M6-1D4 and M6-1E9). L1 ΦTat-CD147gpVIII, L2 ΦSec-CD147gpVIII, L3 ΦTatmut-CD147gpVIII, L4 VCSM13 phage. The immunoreactive bands were visualized by the chemiluminescence substrate detection system. Molecular weight markers (in kilodaltons) are indicated. Phages were prepared from a culture supernatant by standard PEG/NaCl precipitation method

PAGE in reducing conditions, electroblotted, and probed with pooled CD147 mAb (M6-1D4 and M6-1E9). An immunoreactive band with a molecular weight of 28 kDa was visualized (Fig. 4). The band was considered a fusion protein of CD147Ex (20 kDa) and gpVIII (6 kDa) (Intasai et al. 2003). No reactive band was detected in the control lane wherein VCSM13 phages were used.

Discussion

The delivery of proteins across the cytoplasmic membrane into the periplasm of Escherichia coli has been applied in the production of a number of heterologous proteins. The oxidizing environment in the periplasm promotes disulfide bond formation. The vast majority of proteins are exported by the Sec pathway, which is therefore responsible for the targeting and assembly of most proteins in phage display. However, not every recombinant protein can be successfully inserted into the phage particle. Chimeric proteins that included large peptides or stretches of hydrophobic residues acting as stop-transfer sequences, which might be prevented from crossing the membrane, resulted in their inability to be displayed on their surfaces. To alleviate this problem, various methods, such as the modulation of culturing conditions (Chappel et al. 1998; Soltes et al. 2003) and the coexpression of chaperones involved in translocation, have been applied (Bothmann and Pluckthun 1998; DeLisa et al. 2004). However, other factors (i.e., folding kinetics of individual molecules) have not been solved. The Sec channel would not facilitate expressed proteins that completely fold in the cytoplasm.

In 1998, an alternative Sec system, the Tat system, was reported (Weiner et al. 1998). The translocation of active green fluorescence protein via the Tat pathway, which previously failed with Sec machinery, has been described (Thomas et al. 2001). Therefore, the Tat pathway may be useful in the phage display system. In this study, the external domain of the CD147 molecule was selected as a candidate of a TorA twin-arginine leader fusion protein. The novel phagemid pTat8-CD147, which contained the TorA signal sequence, was constructed to employ the Tat machinery for targeting and translocation to facilitate the display of CD147Ex.

The occurrence of CD147 epitopes was evaluated for five mAb by Sandwich ELISA, with HRP-conjugated antigpVIII mAb as tracer (Fig. 2). This system detected CD147 epitopes presented on phage particles and free-form CD147Ex-gpVIII. As hypothesized, CD147Ex-gpVIII fusion protein secreted through the Tat machinery showed a higher positive reactivity with all the anti-CD147 mAb when compared with that delivered via the Sec pathway. The folding of two distinct epitopes of CD147 delivered via the Tat pathway was more efficient, as demonstrated by M6-2B1 and M6-2F9. Interestingly, a strong positive signal was also obtained from the TG-1 Ä*tatABC* mutant transformed with pTat8-CD147. Even though *tat* was deleted, the TorA-CD147Ex-gpVIII fusion protein could pass through the membrane by a nonspecific pathway.

We further investigated whether the positive signal was due to the Sec or the phage-anchoring form of CD147ExgpVIII. To address this question, Sandwich ELISA, using the biotinylated anti-gpIII mAb/HRP-conjugated antibiotin detection system, was used to evaluate the expression of CD147Ex on the phage surface. The absorbance values obtained from ΦTat-CD147gpVIII and ÖSec-CD147gpVIII were considerably different in most of the mAb tested. Since the positive signal determined the phage-bound form of CD147Ex, the number of CD147Ex to be higher than that in ΦSec-CD147gpVIII. Since gpVIII's size is small, we presumed that the structure of gpVIII, along with its fusion partner CD147Ex, might be distorted upon folding. Consequently, the transformed gpVIII lost its efficiency in anchoring into the inner membrane, and thus was unable to assemble into the phage particle. For ΦTatmut-CD147gpVIII, there was no binding of phage to the solid phase coated with mAb. In contrast, Tatmut-CD147gpVIII showed a binding activity comparable with that of ΦTat-CD147gpVIII when detected with the HRP-conjugated anti-gpVIII mAb detection system. We speculated that, after the TG-1 $\Delta tatABC$ mutant was infected with the VCSM13 helper phage, the recombinant phage progeny could not be generated. This finding corresponds to former studies describing defects in the integrity of the E. coli tat mutant outer membrane (Bruser and Sanders 2003; Ize et al. 2003). tat mutants showed leakage of periplasmic protein, while the wild-type E. coli did not (Stanley et al. 2001). Regarding periplasmic leakage and defects of the outer membrane, CD147ExgpVIII fusion proteins that accumulated in the cytoplasm as well as in the cytoplasmic membrane were directly released to a culture supernatant. Since they did not pass through a specific targeting/translocation system, CD147ExgpVIII was not inserted into the inner membrane. Hence, the majority of CD147Ex-gpVIII detected in the culture medium from the Δtat strain were in a phage-nonpackaging form. Therefore, TorA-CD147Ex-gpVIII could be translocated to the periplasm and integrated into the membrane only via a complete Tat machinery. This phenomenon could be confirmed by normal phage biology, as the progeny phage will gather only gpVIII, which are translocated by a specific pathway and correctly integrated into the membrane.

Very recently, Paschke and Hohne (2005) used the Tat pathway for delivering a protein of interest to link to the phage particle. The fusion partner of the displayed polypeptide in this study was not gpVIII, but Fos. Consequently, the exported protein was distributed in the periplasmic space in soluble form. In contrast, our findings demonstrate the incorporation of a Tat-delivered heterologous protein into phage with the fusion partner gpVIII, which contains a hydrophobic region for incorporation into the *E. coli* inner membrane. Our observations here further support the idea that the Tat translocase is involved in membrane protein insertion (Hatzixanthis et al. 2003).

The CD147Ex-gpVIII fusion protein in phage solutions was also identified by Western immunoblotting. The correct

size of the CD147 fusion protein at 28 kDa was observed from ΦTat-CD147gpVIII and ÖSec-CD147gp VIII, which was identical to ΦSec-CD147gpVIII in our previous study (Intasai et al. 2003). The immature polypeptide band did not appear on the membrane. This result confirmed the suitable delivery of expressed TorA-CD147-gpVIII and the specific processing of the TorA signal peptide. The reactive band at 28 kDa also appeared in the lane loaded with ΦTatmut-CD147gpVIII. Regarding this finding and the Sandwich ELISA results (Figs. 2 and 3), the CD147gpVIII contained in the phage preparation from the TG-1 ΔtatABC mutant culture was in free form. Although nonspecifically accessing the periplasm, the TorA signal peptide was apparently removed from the recombinant molecule.

Various functional proteins, such as antibody fragments (Fab and scFv) (Hoogenboom et al. 1991), human growth hormones (Bass et al. 1990), and tissue plasminogen activator derivatives (Manosroi et al. 2001), have been successfully displayed on phage particles. Proteins or peptides are fused to either gpVIII or gpIII. Generally, gpIII is the protein of choice for most phage displays due to its tolerance to large insertions. However, its disadvantage is that less than one copy of recombinant protein is typically displayed per phage particle, and it is not suitable when functional avidity is required. Therefore, a gpVIII phage displaying multivalent molecules is preferred (Sidhu et al. 2000). In our preliminary study, ΦSec-CD147gpVIII—in contrast to ΦSec-CD147gpIII demonstrated binding to U937 cells. However, gpVIII phage display is limited to the length of the insert because a large insert can be less efficiently packaged into the phage. The large insert may possibly affect the initiation of phage assembly by disturbing the interaction between gpVIII and gpVII (Endemann and Model 1995), or it may be too large in diameter to pass through the gpIV exit pore in the outer membrane (Marciano et al. 1999). Recently, phage shock protein PspA was described in relation to enhancing the efficiency of protein transportation via the Tat machinery (DeLisa et al. 2004). While the precise function of PspA is not clearly understood, it appears to maintain the proton motive force, which is required in the Tat translocase function under membrane-associated stress conditions, including filamentous phage infection. Overall, the Tat pathway appears more suitable than the Sec pathway in the phage display of CD147Ex via gpVIII. Based on the present data, the Tat pathway can be applied with candidate proteins, which are less efficiently displayed using the conventional phage display.

Here we solved the limitation in using gpVIII as a fusion partner. The multivalent phage displaying the precise structure of CD147Ex is being applied in further studies to uncover its signal transduction and ligand-partner roles. The current findings also identified an alternative route of fusion protein exportation for packaging into the phage particle, which is normally transported through Sec components. Moreover, while the structural domains of the CD147Ex molecule are homologous to immunoglobulin, expression by pTat8 could improve the quality of antibody libraries. This approach may overcome the aggregation that results in the nonsecretion of ScFv or Fab and, thus, nonattachment to

phage particles. Consequently, the possibility of obtaining reactive clones in the panning step will be increased.

Acknowledgements We are grateful to Dr. Nicole Ngo (The Perinatal HIV Prevention Trial Group, Chiang Mai, Thailand) for cooperation in determining the inserted fragment in pTat8-CD147Ex and to Mr. Phawin Charoensook for technical assistance. We also acknowledge Dr. Ian Thomas and Mr. Brian William Habbard for critical reading of this manuscript.

References

Barbas CF, Burton DR, Scott JK, Silverman GJ (2001) Phage display: a laboratory manual. Cold Spring Harbor Laboratory Press, New York

Bass S, Greene R, Wells JA (1990) Hormone phage: an enrichment method for variant proteins with altered binding properties. Proteins 8:309-314

Berks BC (1996) A common export pathway for proteins binding complex redox cofactors? Mol Microbiol 22:393-404

Berks BC, Sargent F, Palmer T (2000) The Tat protein export pathway. Mol Microbiol 35:260-274

Biswas C, Zhang Y, DeCastro R, Guo H, Nakamura T, Kataoka H, Nabeshima K (1995) The human tumor cell-derived collagenase stimulatory factor (renamed EMMPRIN) is a member of the immunoglobulin superfamily. Cancer Res 55:434-439

Bothmann H, Pluckthun A (1998) Selection for a periplasmic factor improving phage display and functional periplasmic expression. Nat Biotechnol 16:376–380

Bruser T, Sanders C (2003) An alternative model of the twin arginine translocation system. Microbiol Res 158:7-17

Chappel JA, He M, Kang AŠ (1998) Modulation of antibody display on M13 filamentous phage. J Immunol Methods 221:25-34 Danese PN, Silhavy TJ (1998) Targeting and assembly of periplas-

Danese PN, Silhavy TJ (1998) Targeting and assembly of periplasmic and outer-membrane proteins in *Escherichia coli*. Annu Rev Genet 32:59-94

DeLisa MP, Lee P, Palmer T, Georgiou G (2004) Phage shock protein PspA of *Escherichia coli* relieves saturation of protein export via the Tat pathway. J Bacteriol 186:366-373

Endemann H, Model P (1995) Location of filamentous phage minor coat proteins in phage and in infected cells. J Mol Biol 250:496-506

Hatzixanthis K, Palmer T, Sargent F (2003) A subset of bacterial inner membrane proteins integrated by the twin-arginine translocase. Mol Microbiol 49:1377-1390

Heyd B, Pecorari F, Collinet B, Adjadj E, Desmadril M, Minard P (2003) In vitro evolution of the binding specificity of neocarzinostatin, an enediyne-binding chromoprotein. Biochemistry 42:5674-5683

Hoogenboom HR, Griffiths AD, Johnson KS, Chiswell DJ, Hudson P, Winter G (1991) Multi-subunit proteins on the surface of filamentous phage: methodologies for displaying antibody (Fab) heavy and light chains. Nucleic Acids Res 19:4133-4137

Intasai N, Arooncharus P, Kasinrerk W, Tayapiwatana C (2003) Construction of high-density display of CD147 ectodomain on VCSM13 phage via gpVIII: effects of temperature, IPTG, and helper phage infection-period. Protein Expr Purif 32:323-331

Ize B, Stanley NR, Buchanan G, Palmer T (2003) Role of the Escherichia coli Tat pathway in outer membrane integrity. Mol Microbiol 48:1183-1193

Kasinrerk W, Fiebiger E, Stefanova I, Baumruker T, Knapp W, Stockinger H (1992) Human leukocyte activation antigen M6, a member of the Ig superfamily, is the species homologue of rat OX-47, mouse basigin, and chicken HT7 molecule. J Immunol 149:847-854

Kasinrerk W, Tokrasinwit N, Phunpae P (1999) CD147 monoclonal antibodies induce homotypic cell aggregation of monocytic cell line U937 via LFA-1/ICAM-1 pathway. Immunology 96:184–192

Manosroi J, Tayapiwatana C, Gotz F, Werner RG, Manosroi A (2001) Secretion of active recombinant human tissue plasminogen activator derivatives in Escherichia coli. Appl Environ Microbiol 67:2657-2664

Marciano DK, Russel M, Simon SM (1999) An aqueous channel for filamentous phage export. Science 284:1516-1519

Mitraki A, Fane B, Haase-Pettingell C, Sturtevant J, King J (1991) Global suppression of protein folding defects and inclusion body formation. Science 253:54-58
Paschke M, Hohne W (2005) A twin-arginine translocation (Tat)-

mediated phage display system. Gene 350:79-88

Pugsley AP (1993) The complete general secretory pathway in gram-negative bacteria. Microbiol Rev 57:50-108

Sambasivarao D, Dawson HA, Zhang G, Shaw G, Hu J, Weiner JH (2001) Investigation of Escherichia coli dimethyl sulfoxide reductase assembly and processing in strains defective for the sec-independent protein translocation system membrane targeting and translocation. J Biol Chem 276:20167-20174

Santini CL, Ize B, Chanal A, Muller M, Giordano G, Wu LF (1998) A novel sec-independent periplasmic protein translocation pathway in Escherichia coli. EMBO J 17:101-112

Sargent F, Bogsch EG, Stanley NR, Wexler M, Robinson C, Berks BC, Palmer T (1998) Overlapping functions of components of a bacterial Sec-independent protein export pathway. EMBO J 17:3640-3650

Sidhu SS, Weiss GA, Wells JA (2000) High copy display of large proteins on phage for functional selections. J Mol Biol 296:487-495

Soltes G, Barker H, Marmai K, Pun E, Yuen A, Wiersma EJ (2003) A new helper phage and phagemid vector system improves viral display of antibody Fab fragments and avoids propagation of insert-less virions. J Immunol Methods 274:233-244

Stanley NR, Findlay K, Berks BC, Palmer T (2001) Escherichia coli strains blocked in Tat-dependent protein export exhibit pleio-

tropic defects in the cell envelope. J Bacteriol 183:139-144
Tayapiwatana C, Kasinrerk W (2002) Construction and characterization of phage-displayed leukocyte surface molecule CD99. Appl Microbiol Biotechnol 60:336-341

Thomas JD, Daniel RA, Errington J, Robinson C (2001) Export of active green fluorescent protein to the periplasm by the twinarginine translocase (Tat) pathway in Escherichia coli. Mol Microbiol 39:47-53

Vallejo LF, Rinas U (2004) Strategies for the recovery of active proteins through refolding of bacterial inclusion body proteins.

Microb Cell Fact 3:11

Weiner JH, Bilous PT, Shaw GM, Lubitz SP, Frost L, Thomas GH, Cole JA, Turner RJ (1998). A novel and ubiquitous system for membrane targeting and secretion of cofactor-containing proteins. Cell 93:93-101

Binding of multivalent CD147 phage induces apoptosis of U937 cells

Nutjeera Intasai^{1,2,3}, Sabine Mai², Watchara Kasinrerk^{4,5} and Chatchai Tayapiwatana⁴

¹Department of Clinical Microbiology, Faculty of Medical Technology, Mahidol University, Bangkok 10700, Thailand ²Department of Physiology, Manitoba Institutes of Cell Biology, CancerCare Manitoba, University of Manitoba, Winnipeg R3E 0V9. Canada

³Division of Clinical Microscopy and ⁴Division of Clinical Immunology, Department of Medical Technology, Faculty of Associated Medical Sciences, Chiang Mai University, Chiang Mai 50200, Thailand

⁵Medical Biotechnology Unit, National Center for Genetic Engineering and Biotechnology, National Science and Technology Development Agency, Faculty of Associated Medical Sciences, Chiang Mai University, Chiang Mai 50200, Thailand

Keywords: caspase-3, cell signaling, ligand-receptor interaction, phage display, prokaryotic expression

Abstract

CD147 is a broadly expressed cell-surface molecule and serves as a signaling receptor for extracellular cyclophilins. CD147 also appears to interact with immune cells, but its counter-receptor on these cells has not been clearly described. In the present report, we displayed multiple copies of the CD147 extracellular domain (CD147Ex) on VCSM13 phage to study the interaction of CD147 with its ligand. Recognition of phage containing fusion protein of CD147Ex and gpVIII (CD147Ex phage) by four different anti-CD147 mAbs indicated that at least parts of the CD147 are properly folded. Specific binding of CD147Ex phage to various cell types was demonstrated by flow cytometry. Morphological changes, however, were observed only in U937, a monocytic cell line, after 24 h incubation with multivalent CD147Ex phage. After 48 h, U937 cell propagation ceased. Staining with annexin V and the presence of cleaved caspase-3 indicated that many of the CD147Ex phage-treated cells had lost viability through apoptotic cell death. The above results suggest that CD147 induces apoptosis in U973 cells and that at least a portion of this cell death program involves a caspase-dependent pathway.

Introduction

The human leukocyte surface molecule CD147 is a 50- to 60-kDa type 1 transmembrane glycoprotein that belongs to the Ig superfamily (1). CD147 is composed of two Ig domains in the extracellular region, a single transmembrane domain and a short cytoplasmic domain (2-4). The extracellular region contains three glycosylation sites (4), but the glycan portion of the molecule differs according to cell and tissue types. Thus, the different glycosylation patterns of the 27-kDa core protein results in its variable molecular weight (2). The CD147 molecule, also known as EMMPRIN (2), basigin (3, 5) and M6 Ag (6), is broadly expressed on both hematopoietic and non-hematopoietic cells. Expression of CD147 on T cells depends on the differentiation state: it is expressed at higher levels on the cell surface of immature thymocytes than on mature peripheral T cells (7). CD147 expression is up-regulated on activated T cells (2, 3). High expression of CD147 is also observed on human tumor cells (8-10) and seems to be responsible for stimulating fibroblast matrix metalloproteinases

(MMPs) production leading to extracellular matrix degradation, which results in tumor growth and metastasis (11, 12). Some CD147 mAbs inhibited homotypic aggregation of the estrogen-dependent breast cancer cell line, MCF-7, as well as MCF-7 cell adhesion to type IV collagen, fibronectin and laminin (1). Certain CD147 mAbs also induced homotypic cell aggregation of a monocytic cell line, U937 (13). This activation depends upon the activation of protein kinases and re-organization of the cytoskeleton (14). Treatment of immature fetal thymocytes by CD147 mAbs caused aggregation of their CD147 molecules and inhibited their further development into mature T cells (15). Enhancement of mixed lymphocyte responses in CD147 knockout mice indicates a negative regulatory function of CD147 in T cells (16). Triggering of CD147 molecules on T cells by an inhibitory mAb resulted in modulation of lipid rafts, impaired signaling and resulted in impaired expression of the IL-2R α chain CD25 (17).

Received 13 July 2005, accepted 27 April 2006

Correspondence to: C. Tayapiwatana; E-mail: asimi002@chiangmai.ac.th and W. Kasinrerk; E-mail: watchara@chiangmai.ac.th

Transmitting editor. D. Wallach

Advance Access publication 1 June 2006

Most functional studies of CD147 have relied on specific mAbs to induce the cells of interest (11–17). The use of mAbs to mimic native ligand-receptor signaling, however, did not verify the role of CD147 in binding to a membrane ligand to initiate signal transduction. Recently, purified native CD147 was shown to induce the production of secreted MMP-1 by human dermal fibroblasts as well as MMP-2 by a breast carcinoma cell line (MDA-435) (18). The binding affinity of CD147 for its ligand is presumably weak, as is typical for lg superfamily proteins (18).

Phage display technology is a powerful technique for presenting proteins or peptides and has been widely used to identify ligands that bind to a protein of interest (19, 20). However, glycosylation and oligomerization of expressed proteins are not achieved by this technique, and some domains may not fold properly. In an attempt to study the CD147-ligand interaction, we first generated phage-displayed CD147 fused to the minor coat protein, gpIII (21). However, this phage did not bind to cells (unpublished results), indicating a lack of receptor activity. Expression of gpIII fusion protein is restricted to less than one molecule per phage particle (22). Since many molecules of the major coat protein, gpVIII, are present on the phage particle, we have now constructed a multivalent phage displaying the CD147 extracellular domain (CD147Ex) via fusion with the major coat protein, gpVIII (CD147Ex phage) (23). Multiple CD147 molecules on phage particles may enhance binding avidity by multivalent ligand interactions and mimic the ligand-receptor interaction in functional studies of CD147.

In the present study, the function of CD147 was investigated using phage display of CD147. We found that multivalent CD147Ex phage bound to, and induced the apoptotic cell death of, the monocytic cell line, U937. We address here the possible role of the CD147-ligand interaction on the induction of apoptosis.

Methods

Cells and cell lines

The human monocytic cell line (U937), T cell lines (Jurkat and Moit4) and a B cell line (Daudi), acute myelogenous leukemic cell line (KG1a) and T cell lymphoma (HUT78) were maintained in RPMI 1640 medium (GIBCO, Grand Island, NY, USA) supplemented with 10% fetal bovine serum (FBS) (GIBCO), 40 μ g ml⁻¹ gentamicin and 2.5 μ g ml⁻¹ amphotericin B in a humidified atmosphere of 5% CO₂ at 37°C. The BW5147 mouse thymoma cell line was maintained in the same medium and culture conditions.

PBMCs were obtained from healthy donors by Ficoli-Hypaque density gradient centrifugation (Pharmacia Biotech, Uppsala, Sweden).

Multivalent CD147Ex phage preparation

A phage displaying multiple copies of the CD147Ex via the major coat protein, gpVIII, was produced as previously reported (23). Briefly, a DNA encoding CD147Ex fragment was amplified from the mammalian expression vector, pCDM8-CD147 (6). After amplification, the 550-bp PCR product of CD147Ex was inserted into the pComb8 phagemid

(kindly provided by C. F. Barbas, Scripps Institute, USA) to construct pComb8-CD147Ex, a phagemid expressing the CD147Ex. The pComb8-CD147Ex was transformed into TG1 Escherichia coli host strain [supE hsdΔ5 thiΔ(lac-proAB) $F'(traD36proAB+, lacl^q lacZ\Delta M15)$] (kindly provided by A. D. Griffiths, MRC Cambridge, UK). The pComb8-CD147Extransformed E. coli were grown at 25°C with simultaneous isopropyl-β-p-thiogalactopyranoside stimulation and VCSM13 phage infection. Phage particles containing CD147 were detected by sandwich ELISA (23). Four different anti-CD147 mAbs (M6-1B9, IgG3; M6-1E9, IgG2a; M6-1D4, IgM and M6-2F9, IgM) (13, 14) were used as capture antibodies, and HRP-conjugated anti-gpVIII mAb (Amersham Pharmacia Biotech, Buckinghamshire, UK) was used to detect these phage particles.

Identification of CD147Ex phage binding to various cell lines by flow cytometry

Fifty microliters of 6×10^{11} tu ml $^{-1}$ multivalent CD147Ex phages or VCSM13 control phages in RPMI 1640 were mixed with 50 μ l of 10^7 cells ml $^{-1}$ for each cell line tested, and the mixture was incubated on ice for 30 min. The incubated cells were centrifuged at 12 000 rpm for 10 s and the supernatant was discarded. Cells were re-suspended in 50 μ l RPMI 1640 containing anti-gpVIII mAb (10 μ g ml $^{-1}$; Amersham) and incubated on ice for 30 min. After incubation, cells were centrifuged and the supernatant was discarded. Cells were then stained with FITC-conjugated anti-mouse Ig (Silenus, Melbourne, Australia) in RPMI 1640 and incubated on ice for 30 min. After centrifugation and aspiration of the supernatant, the cells were re-suspended in PBS. Flow cytometric analysis was carried out on a FACSCalibur (BD Biosciences, San Jose, CA, USA) using CellQuest software (BD Biosciences).

Confirmation of CD147Ex phage binding to U937 cells by immunocytochemistry

Three milliliters of 1010 tu ml-1 CD147Ex phage or VCSM13 phage in RPMI 1640 were added to 3 ml of 3×10^5 U937 cells ml-1 in RPMI 1640-20% FBS, and the mixture was incubated at 37°C for 24 h in a 5% CO2 atmosphere. After incubation and low-speed centrifugation and re-suspension in a smaller volume, 100 μ l of 1 \times 10 6 cells ml $^{-1}$ phage-incubated U937 cells were placed on a silane-coated slide, air dried, and fixed with 3.7% formaldehyde in PBS containing 50 mM MgCl₂ for 10 min. Slides were washed three times in PBS containing 50 mM MgCl₂ and blocked with 1% BSA in saline sodium citrate (SSC) at room temperature for 5 min. Anti-gpVIII mAb (Amersham) was added and incubated at room temperature for 1 h. After washing, Alexa680-conjugated goat anti-mouse Ig (Molecular Probes, Eugene, OR, USA) was added to the slide and incubated at room temperature for 30 min. After washing, U937 nuclei were counterstained with 4',6-diamidino-2-phenylindole (DAPI) (Molecular Probes). Image analysis was carried out using the Spectra Cube (Applied Spectral Imaging, Carlsbad, CA, USA) on a Zeiss Axiophot 2 microscope (Carl Zeiss Canada Ltd., Toronto, Ontario, Canada) and the SKYVIEW 2.1.1 software (Applied Spectral Imaging). After spectral image acquisition, the acquired spectral image was classified using the combinatorial table containing the

fluorochrome combinations for the above analyses (24). This classified image was generated to delineate the cleaved caspase-3 positive area (classified in red). Inverted DAPI images represent nuclei.

Effect of CD147Ex phage on various cell types

One hundred microliters of 1010 tu ml-1 CD147Ex phage in RPMI 1640 was added to 100 μ l of 3 \times 10⁵ cells ml⁻¹ of each cell type in RPMI 1640-20% FBS in the wells of a 96-well flatbottom tissue culture plate (NUNC, Roskilde, Denmark) and the mixture was incubated at 37°C in a 5% CO2 incubator. VCSM13 phage and phage-displayed green fluorescent protein were used as controls. Live cultures were observed at 1, 2, 3, 4, 8, 24 and 48 h of incubation. Images were taken under a Zeiss Axiovert 100 microscope (Zeiss).

Antibody neutralization of CD147Ex phage in U937 cell death induction

One hundred microliters of 1010 tu ml-1 CD147Ex phage in RPMI 1640 were pre-incubated with 10 μg mI⁻¹ anti-CD147 mAbs, M6-14D and M6-2F9, at 37°C for 30 min. The mixture was added to 100 μ l of 3 \times 10⁵ cells ml⁻¹ of each cell type in RPMI 1640~20% FBS in a 96-well flat-bottom tissue culture plate (NUNC) and incubated at 37°C in a 5% CO2 incubator. The cultures were observed at 1, 2, 3, 4, 8, 24 and 48 h of incubation. Images were taken under a Zeiss Axiovert 100 microscope (Zeiss).

Cytotoxicity assay

CD147Ex phage-induced U937 cell death was investigated by mixing 3 ml of 1010 tu ml-1 multivalent CD147Ex phage or VCSM13 phage re-suspended in RPMI 1640 with 3 ml of $3 \times 10^5 \, \mathrm{U}937 \, \mathrm{cells} \, \mathrm{ml}^{-1}$ in RPMI 1640-20% FBS, and incubating for 48 h at 37°C in a 5% CO2 incubator. After washing, cells were stained using the LIVE/DEAD Viability/Cytotoxicity Kit (Molecular Probes) according to the manufacturer's instructions. Stained cells were washed twice and cytospun onto microscope slides at a density of 105 cells per slide. Nuclei were counterstained with DAPI (Molecular Probes). Images were taken using a Zeiss Axioplan2 microscope (Zeiss) and FITC (excitation at 494 nm, emission at 518 nm), Texas red (excitation at 595 nm, emission at 620 nm) and DAPI (excitation at 359 nm, emission at 461 nm) filters (Zeiss). The fluorescence intensity was analyzed by Northern Eclipse 5.0 (Empix Imaging Inc., Mississauga, Ontario, Canada) using the NucDen function.

Annexin V assay

U937-CD147Ex phage incubation was performed as described for the cytotoxicity assay. VCSM13 phage and phage-displayed survivin (SVV) were included as controls. After incubation, incubated U937 cells were washed with cold PBS and re-suspended in 100 µl of binding buffer (10 mM HEPES pH 7.4, 140 mM NaCl, 2.5 mM CaCl₂). One hundred microliters of 106 cells ml-1 of phage-incubated U937 cells were incubated with 5 µl annexin V conjugated with FITC (BD Biosciences) for 15 min at room temperature in the dark. Two microliters of propidium iodide (PI, 50 µg ml⁻¹) were added to the incubated cells. Flow cytometric analysis was carried out

within 1 h on a FACSSort (BD Biosciences) using CellQuest software (BD Biosciences).

Examination of cleaved caspase-3 by flow cytometry

Incubation of U937 cells with CD147Ex phage was performed as described previously in the cytotoxicity assay. VCSM13 phage and cisplatin (Sigma-Aldrich, St Louis, MO, USA) were included as controls. After incubation, U937 cells were harvested, washed and re-suspended in PBS. Methanol-free formaldehyde was then added to the re-suspended cells to a final concentration of 0.25%, incubated at 37°C for 10 min and placed on ice for 1 min. The cells were then permeabilized with ice-cold 90% methanol and incubated on ice for 30 min. One million permeabilized cells were washed twice with 0.5% BSA in PBS and re-suspended in the same buffer. Cells were subsequently incubated with rabbit anti-cleaved caspase-3 (ASP175) (5A1) mAb (Cell Signaling, Beverly, MA, USA) at room temperature for 30 min. Cells were then stained with Alexa488-conjugated anti-rabbit lg antibody (Molecular Probes) at room temperature for 30 min. After incubation, cells were washed and re-suspended with 500 µl of 0.5% BSA in PBS. Flow cytometric analysis was performed on a Beckman Coulter EPICS ALTRA (Beckman Coulter, Fullerton, CA, USA).

Detection of cleaved caspase-3 by immunocytochemistry

U937 cells were incubated with CD147Ex phage for 48 h as described in the cytotoxicity assay. VCSM13 phage and cisplatin (Sigma-Aldrich) were included as controls. After 48 h incubation, cells were fixed for 10 min with 3.7% formaldehyde in PBS containing 50 mM MgCl₂. Fifty microliters of 1 × 10⁶ cells ml-1 fixed cells were placed on a silane-coated slide and air dried. The slides were fixed with 3.7% formaldehyde in PBS containing 50 mM MgCl₂ for 10 min. Following washing, cells were permeabilized with 0.2% Triton-X 100 for 12 min. Slides were then washed in PBS containing 50 mM MgCl2 and blocked with 1% BSA in SSC at room temperature for 5 min. Then, the fixed cells were incubated with rabbit anti-cleaved caspase-3 (ASP175) (5A1) mAb (Cell Signaling) at 4°C overnight. After washing, cells were blocked and then incubated with Alexa680-conjugated goat anti-rabbit IgG antibody (Molecular Probes) at room temperature for 30 min. U937 nuclei were counterstained with DAPI. Image analysis was carried out using the Spectra Cube (Applied Spectral Imaging) on a Zeiss Axiophot 2 microscope (Zeiss) and the SKYVIEW 2.1.1 software (Applied Spectral Imaging). Spectral, classified and inverted images are generated as described previously.

Analysis of nuclear translocation of apoptosis-inducing factor by western blot

U937 cells were incubated for 24 h with CD147Ex phage as described previously. VCSM13 phage and phage-displayed SVV were used as controls. Nuclear and cytoplasmic fractions were extracted using NE-PER® Nuclear and Cytoplasmic Extraction Reagents (Pierce Biotechnology, Perbio Science, France). Protein content was quantified by a modified Lowry assay. Eighty micrograms of total protein from cell lysates were resolved on 12.5% SDS-PAGE under reducing conditions, and then electroblotted onto a polyvinylidene fluoride membrane

(PALL, East Hills, NY, USA). The membrane was blocked at room temperature for 2 h in 5% skimmed milk in Tris-buffered saline (TBS) pH 7.6, and then incubated with rabbit anti-apoptosis-inducing factor (AIF) antibody (Cell Signaling), which recognizes both a precursor form of AIF at 67 kDa and a mature form of AIF at 57 kDa, at 4°C overnight on a shaking platform. On the following day, the blot was washed with 0.1% Tween 20 in TBS pH 7.6 and incubated with goat anti-rabbit Ig-HRP at room temperature for 1 h. After washing, the immunoreactive bands were then visualized by the chemiluminescent detection system (Amersham).

Results

Multivalent CD147Ex phage binds to various cell types

Phage expressing multivalent CD147 ectodomain were produced and assayed for display of the CD147 molecules by sandwich ELISA using four separate anti-CD147 mAbs.

sandwich ELISA using four separate anti-CD147 mAbs. Similar to our previous report (23), the CD147Ex phage was recognized by all these anti-CD147 mAbs (data not shown).

To study the interaction of CD147Ex with molecules on the cell surface of various cell types, CD147Ex phage was incubated with each cell type and binding was determined by flow cytometry. The CD147Ex phage bound to all tested human hemotopoietic cell lines including U937, Daudi, Jurkat, Molt4, KG1a and HUT78 as well as BW5147 mouse thymoma cells (Fig. 1). A population of peripheral blood lymphocytes was also shown to exhibit positive reactivity (Fig. 1). In contrast, wild-type phages did not bind to any cell line tested. To confirm the flow cytometric results by a different method, U937 cells were incubated with CD147Ex phages and control phages for 24 h, stained with anti-gpVIII mAb and followed by goat anti-mouse Ig-Alexa680. Binding of CD147Ex phage on U937 cells was also demonstrated by immunocytochemistry (Fig. 2). Interestingly, the CD147Ex phage-binding cells harbored apoptotic bodies (Fig. 2B, arrow).

CD147Ex phage induces morphological changes and inhibits growth of U937 cells

We tested the effects of CD147Ex phages and controls on a variety of cell lines. These included U937, Jurkat, Daudi and

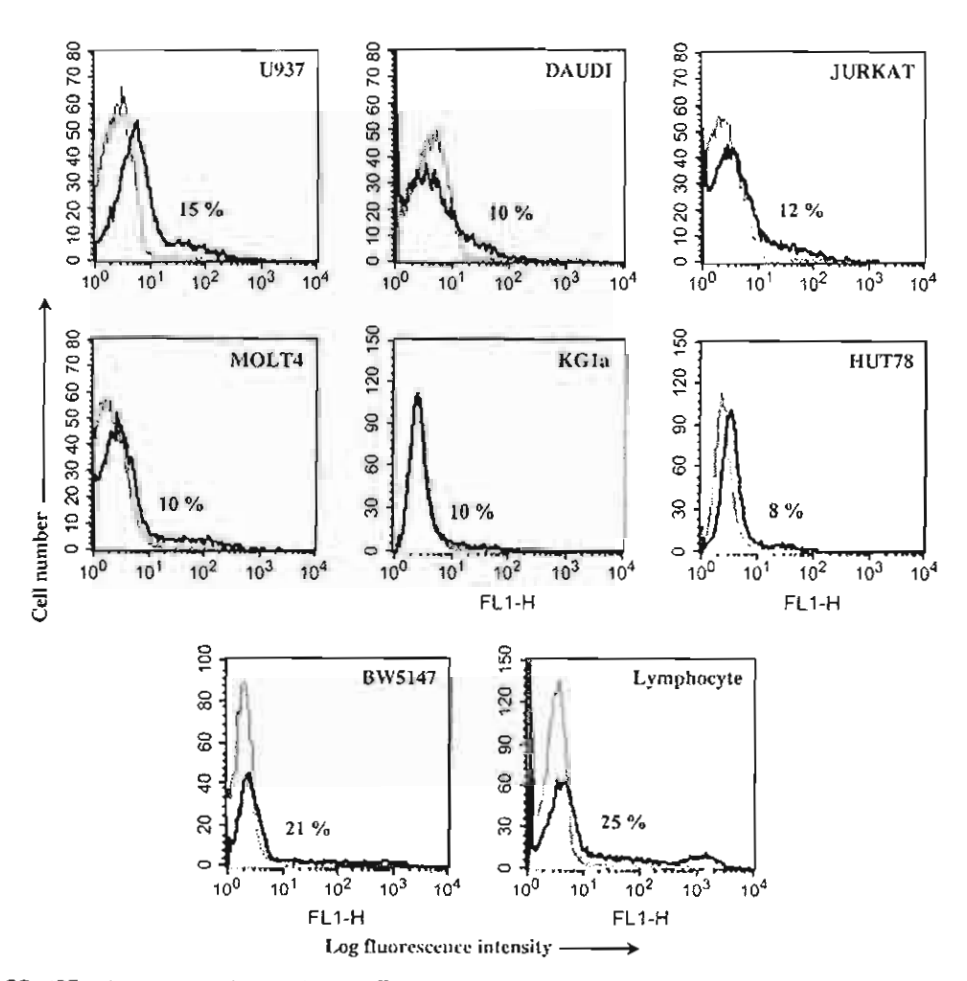


Fig. 1. Binding of CD147Ex phages on various cell types. The cells were incubated with CD147Ex phages (solid lines) and VCSM13 control phages (dotted lines). Cell lines or PBMCs were stained with anti-gpVIII mAb and FITC-conjugated anti-mouse ig antibody. Peripheral blood lymphocytes were gated according to their size and granularity and analyzed for phage binding. The figure shows the percentages of CD147 phage bound cells. Results from one representative experiment of three are shown.

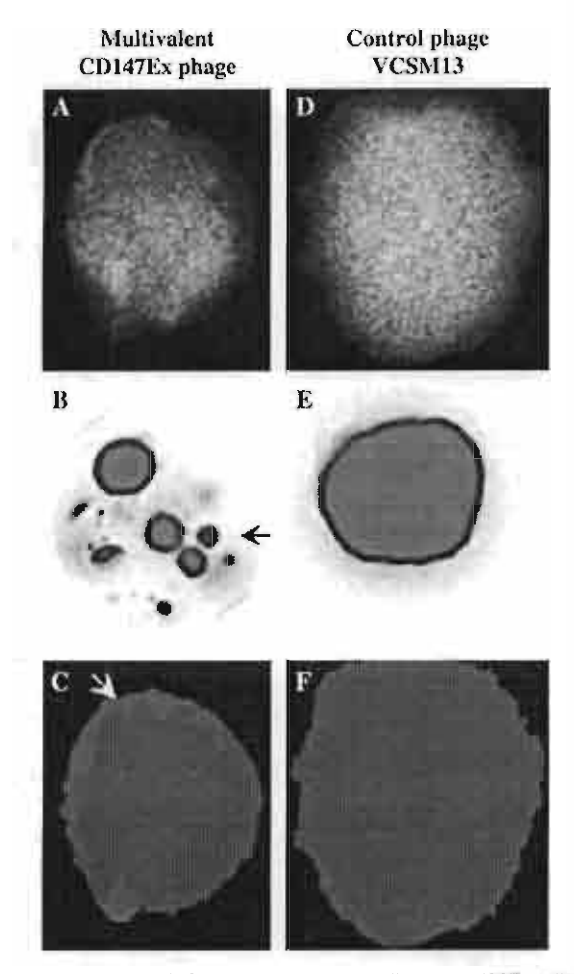


Fig. 2. Detection of CD147Ex phage binding on U937 cells by immunocytochemistry. U937 cells were incubated with recombinant phages or wild-type phages for 24 h, stained with anti-gpVIII mAb followed by goat anti-mouse Ig-Alexa680. The nuclear morphology was verified by DAPI staining. A and D represent spectral mages. B and E represent inverted DAPI and C and F represent classified images in which Alexa680 is designated in red. Black arrow snows the apoptotic bodies and white arrow indicates the binding of CD147Ex phages on U937 cells.

Molt4. Of these tested cell lines, only U937 cells exhibited morphological changes after incubation with CD147Ex phage. Morphological characteristics of apoptotic cell death such as cytoplasmic blebbing and nuclear fragmentation (25) were observed after 24 h of incubation with CD147Ex phages, but not with control phages (Fig. 3A, arrows and Fig. 3B and C, respectively). After a 48 h of incubation, the cell density of U937 cells in wells containing CD147Ex phage (Fig. 3D) was noticeably lower than in wells containing wild-type phages or phage-displayed irrelevant protein (Fig. 3E and F). The U937 cell concentration at the beginning of the experiment was 3×10^5 cells ml 4 . By 48 h, the CD147Ex phage-incubated cells remained at a similar concentration, $2.9 \times 10^5 \pm 0.7 \times$ 105, while the wild-type- and irrelevant protein expressing phage-incubated cells increased to $9.5 \times 10^5 \pm 0.4 \times 10^5$ and $8.4 \times 10^5 \pm 0.8 \times 10^5$ cells ml⁻¹, respectively.

To demonstrate the effect of CD147Ex displayed on phage particles in triggering cell death, anti-CD147 mAbs, M6-1D4 and M6-2F9 were pre-incubated with CD147Ex phages before incubating with U937 cells. Morphological changes of U937 cells were significantly decreased compared with those induced by CD147Ex phages in the absence of CD147 mAb (Fig. 3G and H).

Cytotoxic effect of CD147Ex phage on U937 cells

Since the morphological changes of CD147Ex phageincubated U937 cells suggested that cell death had occurred, vitality and cytotoxicity staining was performed. In the method employed, intracellular esterase activity in live cells converts the non-fluorescent cell-permeable calcein AM to the intensely fluorescent calcein, which is retained within live cells. Ethidium homodimer (EthD-1) enters the permeabilized plasma membranes of dead cells and undergoes a 40-fold increase in red fluorescence after binding to nucleic acids. Therefore, the nuclei of the dead cells appear red under the fluorescence microscope. Thus, cells with an active metabolism (calcein positive) that allow EthD-1 to penetrate and stain their nucleic acids most likely correspond to late-state apoptosis (26). We found double staining with calcein and EthD-1 in many recombinant phage-incubated U937 cells (Fig. 4A-C). In contrast, wild-type phage-incubated U937 cells were positive only for calcein (Fig. 4D-F). One hundred cells were examined in three dependent experiments for the fluorescence intensity of calcein and EthD-1. Mean EthD-1 fluorescence intensity of U937 cells when incubated with multivalent CD147Ex phages was 4.4 times higher than that with wild-type phages, while the mean calcein fluorescence intensity from both conditions were not significantly different.

CD147Ex phage induces apoptosis of U937 cells

To confirm that the death of multivalent CD147Ex phageincubated U937 cells is due to apoptosis, the annexin V assay was employed. In the presence of CD147Ex phages, more annexin V-positive cells were observed compared with uninduced and those treated with the wild-type phage and phage-displayed irrelevant protein (Fig. 5). These results suggested that multivalent CD147Ex phage induces apoptotic cell death in U937 cells (27-29).

Involvement of caspase-3 activation in the mechanism of cell death of U937 cells incubated with CD147Ex phages

To assess the mechanism of apoptotic cell death in CD147Ex phage-incubated U937 cells, cleaved caspase-3 was analyzed by flow cytometry. The level of cleaved caspase-3 observed in recombinant phage-incubated U937 cells (Fig. 6, thin line) was higher than wild-type phage-treated U937 cells (Fig. 6, filled histogram). However, the level of cleaved caspase-3 induced by CD147 phage was not as high as that triggered by cisplatin (Fig. 6, thick line). There was no difference in the level of cleaved caspase-3 between wildtype phage-induced U937 cells and un-induced U937 cells (data not shown).

The intracellular cleaved caspase-3 assay was also determined by immunocytochemistry. Un-treated U937 cells and wild-type phage-treated U937 cells were negative for cleaved caspase-3, whereas induction of U937 cells by cisplatin and CD147Ex phage resulted in positive staining (Fig. 7). We noted

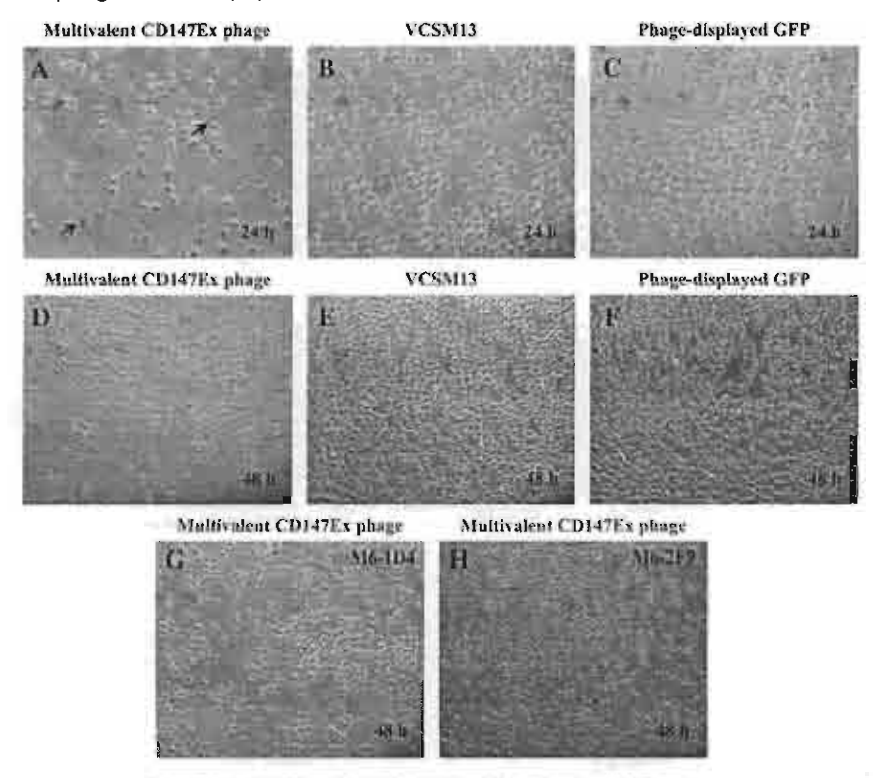


Fig. 3. CD147Ex phages induced morphological change and growth arrest of U937 cells. U937 cells were incubated with (A) CD147Ex phages. (B) VCSM13 phages or (C) phage-displayed green fluorescent protein (GFP) and observed under an inverted microscope (200×). Morphological change of U937 cells was observed after 24 h incubation (arrows). The cell density of U937 cells in wells containing (D) CD147Ex phages was significantly lower than those in the presence of (E) VCSM13 phages and (F) phage-displayed GFP after 48 h of incubation (100×). Morphological change of CD147Ex phage-incubated U937 cells at 24 h of incubation was substantially reduced when pre-incubated CD147Ex phages with anti-CD147 mAbs. (E) M6-1D4 and (F) M6-2F9.

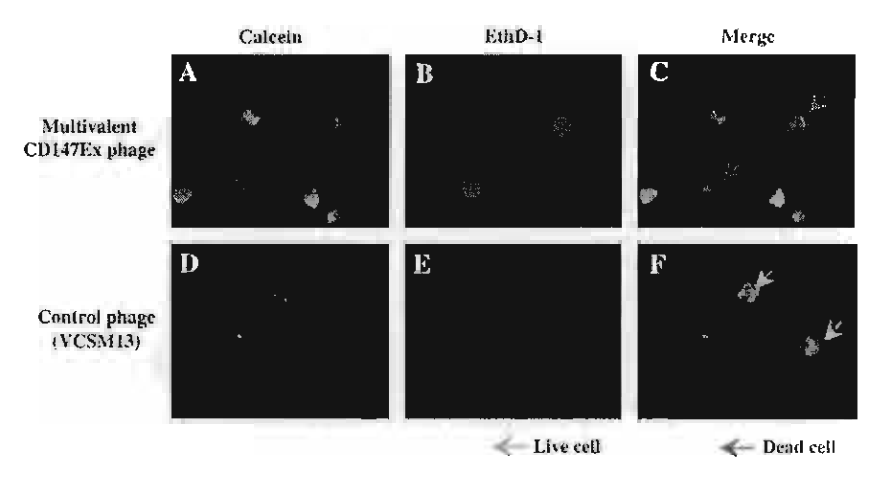
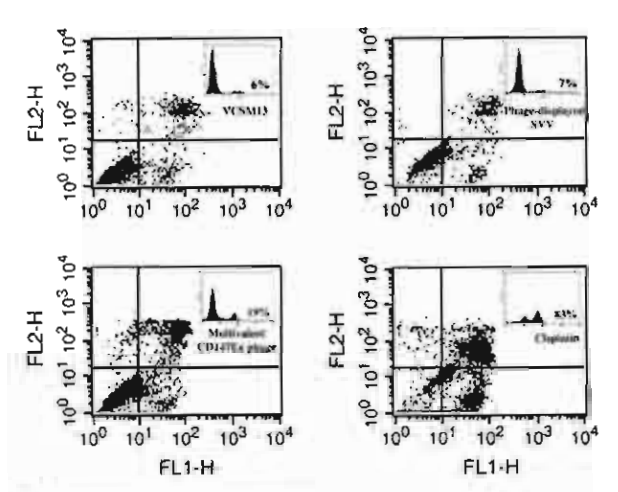


Fig. 4. Cytotoxicity of CD147Ex phages on U937 cells. U937 cells were incubated with (A–C) CD147Ex phages or (D–F) VCSM13 phages for 48 h and stained with LIVE/DEAD Viability/Cytotoxicity reagent. Green arrows indicate live cells and pink arrows represent dead cells. Results are representative of three separate experiments.

that of the CD147Ex phage-treated cells that had apoptotic nuclei, some were positive (Fig. 7L) and some were negative (Fig. 7O) for anti-cleaved caspase-3, whereas all cisplatin-treated cells with apoptotic nuclei were positive for anti-cleaved caspase-3.

AIF is not involved in the death of U937 cells after incubation with CD147Ex phage

AIF is a mitochondrial protein that, upon mitochondrial transmembrane potential $(\Delta \Psi_m)$ loss, is released from mitochondria and translocated into the nucleus (30). To determine the



Flg. 5. Annexin V assay of CD147Ex phage-induced U937 cells. U937 cells were incubated with VCSM13 phages, phage-displayed SVV. CD147Ex phages or cisplatin for 48 h. Cells were incubated with annexin V-FITC and PI and analyzed by flow cytometry. Viable U937 cells are negative for both annexin V and PI; early apoptotic U937 cells are positive for annexin V while being negative for PI; late apoptotic U937 cells are positive for both annexin V and PI and necrotic U937 cells are positive for PI while being negative for annexin V (27–29).

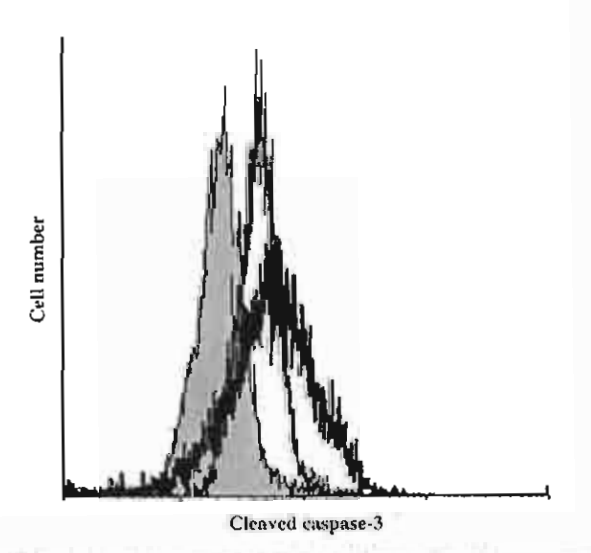


Fig. 6. CD147Ex phage-induced U937 cell death resulted in caspase-3 activation. U937 cells were incubated with CD147Ex phages (thin line), VCSM13 control phages (filled histogram) or cisplatin (thick line) for 48 h. Cleaved caspase-3 was examined by flow cytometry after intracellular staining with rabbit anti-cleaved caspase-3 mAb. Results are representative of two separate experiments.

involvement of AIF in the induction of nuclear apoptosis of CD147Ex phage-treated U937 cells, nuclear and cytoplasmic fractions of CD147Ex phage-treated as well as VCSM13 phage-treated and phage-displayed SVV-treated U937 cells were separated and the western blot analysis was carried out to detect AIF. In un-induced cells, AIF was present primarily as its 67-kDa proform and processed to a 57-kDa mature form when caspase-independent cell death is activated. Nuclear translocation of the 57-kDa AIF did not appear to increase in

CD147Ex phage-treated cells after 24 h incubation (Fig. 8). In contrast, it appeared to be less than in the un-induced cells (Fig. 8).

Correlation between binding of CD147Ex phage to U937 cells and apoptotic nuclei

The binding of CD147Ex phage to individual U937 cells that harbor apoptotic nuclei was examined by immunocytochemistry. Recombinant phage adhering to individual U937 cells was visualized on classified image which is shown in red (Fig. 2A–C). Sixty percent of CD147Ex phage-incubated U937 cells were positively stained with anti-gpVIII mAb, while 42% of CD147Ex phage-incubated U937 cells had apoptotic nuclei. In contrast, anti-gpVIII mAb did not bind to wild-type phage-incubated U937 cells (Fig. 2D–F).

Discussion

After the discovery of the CD147 protein, there was no concrete evidence linking CD147 with the triggering of membrane bound molecules. Although recombinant CD147 could be expressed on the surface of other cell types in vitro. this was not suitable for studying CD147 function in triggering its cell-surface ligands and leads the signal into the cells, as other pairs of membrane protein interactions may counteract or interfere with the signal originating from CD147 induction. To overcome this problem, phage display technology is introduced for this purpose. Hence, we previously generated phage-displayed CD147Ex via gpllI and used it for studying the CD147 function and characterization of CD147 ligands (21). However, the binding of these recombinant phages to cells could not be detected by immunofluorescence. This is most likely due to the level of heterologous CD147 proteins displayed on phage gpIII being restricted to less than one molecule per phage particle (22). High levels of heterologous protein display can be achieved on gpVIII, as each phage particle contains ~2000 copies of the protein (31, 32). Moreover, multivalent CD147 molecules expressed on the 930-nm length filamentous phage might overcome the limitation of CD147 binding to low levels of its ligands on the cell surface. Thus, we decided to generate phage that displayed multivalent CD147Ex on its surface (23). With this new approach, the present study demonstrated the binding of multivalent CD147Ex phages to various cell types and a new function of CD147 has been uncovered for U937 cells.

The physical association between CD147 and β -1 integrin in the membrane has been reported (33, 34). Berditchevski *et al.* (33) suggested that association of $\alpha_3\beta_1$ integrin and $\alpha_6\beta_1$ integrin with CD147 is in lateral fashion, similar to the interaction of β -3 integrins with CD47, another β superfamily protein (35, 36). It has been reported that CD147 also serves as a signaling receptor for extracellular cyclophilin A (37–39). Recently, a cyclophilin-binding region in the CD147 molecule has been identified as the transmembrane domain (40). The proline residue located at position 211 in the transmembrane domain was the critical residue responsible for intracellular interaction of cyclophilins and CD147 (40). Interaction between lactate transporter, MCT1 and CD147 has also been reported (41, 42). Association between MCT1 and fusion

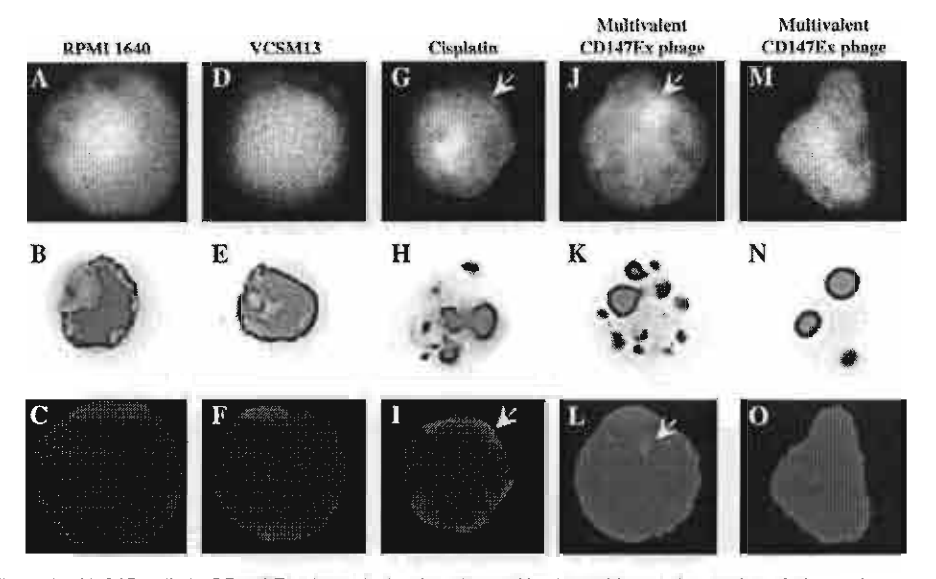
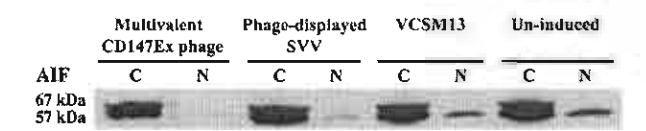


Fig. 7. Apoptotic cell death of U937 cells in CD147Ex phage induction showed both positive and negative of cleaved caspase-3. U937 cells were incubated with RPMI 1640, VCSM13 phage, cisplatin or CD147Ex phages. Cleaved caspase-3 was determined by intracellular staining using rabbit anti-cleaved caspase-3 mAb and goat anti-rabbit IgG-Alexa680. A, D, G, J and M represent spectral images; B, D, H, K and N represent inverted DAPI images and C, F, I, L and O represent classified images, in which Alexa680 is designated in red. Arrows indicate cleaved caspase-3.



Flg. 8. Analysis for nuclear translocation of AIF in CD147Ex phagetreated U937 cells. U937 cells were incubated with RPMI 1640 (uninduced), VCSM13 phages, phage-displayed SVV or CD147Ex phages for 24 h. Nuclear (N) and cytoplasmic proteins (C) were extracted using NE-PER® Nuclear and Cytoplasmic Extraction Reagents. Western blot analysis was performed as described in Methods by using the antibody against AIF.

protein of extracellular domain of CD2 and transmembrane or cytoplasmic domains of CD147 suggested that transmembrane and cytoplasmic domains of CD147 are important for lateral interaction between MCT and CD147 (41). None of these studies have reported interactions of the CD147 external domain with any cell-surface molecule. With our novel approach, only the external domain of CD147 is expressed on phage particles; thus, it is unlikely that integrins, cyclophilins or MCTs are the CD147 ligand. Recently, the possibility that CD147 could be an autoreceptor has been suggested (18). The first extracellular Ig domain of CD147, which contains a glycosylated site, is required for homophilic counterreceptor binding activity (18, 43). In contrast, the CD147 displayed on phage surface was in non-glycosylated form. Thus, it should not interact with the naive CD147 on the cell membrane. This finding suggests further study of the interaction of CD147 with its surface ligand conveying the molecular signals.

Using the tool we developed in this study, we were able to show that triggering U937 cells with multivalent CD147Ex phages resulted in morphological changes, that is, apoptotic nuclei, in contrast to other cell types. Engagement of cell-

surface receptors by multiple ligands might be necessary for signaling. A similar phenomenon has been reported in a study that showed IgE dimers were less effective than larger IgE oligomers in stimulating cellular responses (44). Dependency of cellular responses on receptor aggregates also has been observed for related receptors, such as the B cell receptor (45, 46) and TCR (47, 48). Thus, signal transduction by individual binding of monovalent CD147 may differ from the crosslinking of cell-surface ligands with multivalent phage carrying CD147Ex. Herein, the interaction of multivalent phage displaying CD147Ex and its counter-receptors on U937 cells mediated the morphological changes characteristic of apoptotic cell death. In addition, pre-incubation of CD147Ex phages with anti-CD147 mAbs, M6-1D4 and M6-2F9, significantly reduced the death of U937 cells compared with U937 cells induced by CD147Ex phage only. These mAbs may hinder the epitope that play an important role in death induction of U937 cells. Thus, interactions between CD147Ex on the phage particle and its ligands on U937 cells might consequently lead to death signals. The death of multivalent CD147Ex phage-incubated U937 cells did not result from chemical toxicity of the phage preparation because this phenomenon was not observed when using wild-type phage or phage expressing irrelevant protein. In addition, cell death was specifically observed in U937 cells but not in other tested cell lines. In addition to multivalent CD147Ex phage-induced apoptotic morphological change of U937 cells, growth arrest of U937 cells was observed after 48 h of incubation.

The morphological features indicating apoptotic cell death, that is, double staining with calcein and EthD-1 and double staining with annexin V and PI of U937 cells incubated with the multivalent CD147Ex phage, suggest a possible involvement of caspase activation. To address this question, the presence of cleaved caspase-3 in U937 cells incubated with multivalent

CD147 phage was examined by flow cytometry and immunocytochemistry. The level of cleaved caspase-3 in U937 cells incubated with multivalent CD147Ex phages was higher than in un-induced or wild-type phage-incubated U937 cells. However, it was not as remarkable as levels of cleaved caspase-3 seen in cisplatin-induced U937 cells. When individual U937 cells were analyzed by immunocytochemistry, the percentage of recombinant phage-induced U937 cells harboring apoptotic nuclei was 74.3%, but with only 12.8% containing high level of cleaved caspase-3. Therefore, it is possible that the apoptotic cell death of CD147Ex phageincubated U937 cells is partially explained by an enhancement in cleaved caspase-3 level. The reasons for this differential reaction of U937 cells to CD147Ex phage are currently unknown. This may be resulted from different kinetics of apoptotic induction and/or other pathways of program cell death (PCD). Initiation of caspase-dependent and -independent cell death in response to a given stimulus has been recently reported (49, 50). Triggering of HLA class I molecules on Jurkat T lymphoblasts results in apoptotic cell death induction by two parallel pathways, caspase-dependent and -independent pathways (50). According to current knowledge, one central molecule in caspase-independent cell death is AIF (30). Upon induction of apoptosis, AIF translocates from mitochondria to the nucleus and results in DNA fragmentation and marginal chromatin condensation (30). Thus, analysis of AIF localization in both nuclear and cytoplasmic fractions of U937 cells by western blot was performed earlier than caspase-3 analysis. In this study, we showed that nuclear translocation of AIF in CD147Ex phage-treated U937 cells was not detected, which indicates that a caspase-independent pathway via AIF is not involved in cell death mediated by multivalent CD147. Since caspase-independent pathway is not involved in this study, alternative pathways of PCD may play roles in cleaved caspase-3 negative apoptotic cell death. This may be apoptosis-like or necrosis-like cell death as described for other molecules, that is, bN(P3 (51-53). The cell death resembled apoptosis, as evidenced by outer membranes phosphatidyl serine exposure and apoptotic nuclei, but was cleaved caspase-3 as well as AIF independent. Therefore, it is suggested by our study that the caspasedependent pathway may play a major role of apoptotic cell death in U937 cells after incubation with CD147Ex phage.

Under physiological conditions, interaction of CD147 with its counter-receptor may have a very low affinity with an extremely fast dissociation rate, as has been described for a variety of cell adhesion receptors, such as CD2 with its counterreceptors CD48 and CD58 (54, 55). The functional consequences of the physical association of these cell adhesion molecules with their ligands may also require high polyvalent ligands that are regulated by their expression levels. Thus, it is tempting to speculate that the fast and strong up-regulation and patching of CD147 upon activation of T cells (6, 56) controls its interaction with its counter-receptor. Following CD147 engagement, firm cell contact was established by β-1 and β-2 integrins, which were characterized as physical and functional partners of CD147 (13, 33, 34). Evidence for CD147 as a β-2 integrin amplifier is given by the enhanced adhesiveness of leukocyte function-associated antigen-1 upon CD147 triggering by mAbs (13). The cooperation be-

tween CD147 and integrins is conserved among species as lack of CD147 impairs the integrin-dependent cellular architecture of Drosophila cells (57), Of physiological relevance, we suggest that CD147 may play a fundamental role in the negative regulation of immune responses (17, 58) by induction of apoptosis in the target cells expressed its counter-receptor. This is also consistent with the finding that lymphocytes isolated from CD147-/- knockout mice better proliferate in a mixed lymphocyte reaction than those observed in lymphocytes derived from wild-type mice (59).

In conclusion, we introduce here a useful strategy, applying the phage display technique to study the interaction of cellsurface molecules. A multivalent CD147Ex phage was generated and used in a functional study of the CD147 molecule. The results clearly demonstrated that a CD147 ligand exists on various cell types. A function of CD147 in triggering apoptotic cell death in U937 cells was identified. Since this phenomenon specifically occurred with U937 cells, which is a monocytic cell line, the involvement of CD147 in immune regulation of specific lineage and developmental stages will be the focus of future studies.

Acknowledgements

We gratefully acknowledge Edward Rector for his kind guidance in detection of cleaved caspase-3 by flow cytometry. We are thankful to Sawitree Chiampanichayakul, Umpa Yasamut, Khajornsak Tragoolpua and Wutigri Nimlamool for their technical assistances and Mark E. Peeples for his helpful discussions and critical reading of the manuscript. We are especially grateful to Suttichai Krisanaprakornkil for valuable suggestion in detection of AIF by western blot. This work was supported by the scholarship under the Commission on Higher Education Thai Staff, the Thailand Research Fund and the National Center for Genetic Engineering and Biotechnology (BIOTEC), Thailand and Cariadian Institutes of Health Research Strategic Training Program 'Innovative Technologies in Multidisciplinary Health Research Training', Canada.

Abbreviations

AIF apoptosis-inducing factor CD147Ex CD147 extracellular domain CD147Ex phage containing fusion protein of CD147Ex and gpVIII

phage

DAPI 4'6-diamidino-2-phenylindole EthD-1 ethidium homodimer **FBS** fetal bovine serum MMP matrix metalloproteinase PCD program cell death Pί propidium iodide SSC saline sodium citrate

SVV survivin

TBS Tris-buffered saline

References

1 Staffler, G. and Stockinger, H. 2000, CD147, J. Biol. Regul. Homeost. Agents 14:327

2 Biswas, C., Zhang, Y., DeCastro, R. et al. 1995. The human tumor cell-derived collagenase stimulatory factor (renamed EMMPRIN) is a member of the immunoglobulin superfamily. Cancer Res. 55:434.

3 Miyauchi, T., Masuzawa, Y. and Muramatsu, T. 1991. The basigin group of the immunoglobulin superfamily: complete conservation of a segment in and around transmembrane domains of human

- and mouse basigin and chicken HT7 antigen. J. Biochem. (Tokyo) 110:770.
- 4 Muramatsu, T. and Miyauchi, T. 2003. Basigin (CD147): a multifunctional transmembrane protein involved in reproduction, neural function, inflammation and tumor invasion. *Histol. Histopathol.* 18:981
- 5 Miyauchi T., Kanekura, T., Yamaoka, A., Ozawa, M., Miyazawa, S. and Muramatsu, T. 1990. Basigin, a new, broadly distributed member of the immunoglobulin superfamily, has strong homology with both the immunoglobulin V domain and the beta-chain of major histocompatibility complex class II antigen. J. Biochem. (Tokyo) 107:316.
- 6 Kasinrerk, W., Fiebiger, E., Stefanova, I., Baumruker, T., Knapp, W. and Stockinger, H. 1992. Human leukocyte activation antigen M6, a member of the Ig superfamily, is the species homologue of rat OX-47, mouse basigin, and chicken HT7 molecule. J. Immunol. 140-847
- 7 Kirsch, A. H., Diaz, L. A., Jr, Bonish, B., Antony, P. A. and Fox, D. A. 1997. The pattern of expression of CD147/neurothelin during human T-cell ontogeny as defined by the monoclonal antibody 8D6. Tissue Antigens 50:147.
- 8 Ellis, S. M., Nabeshima, K. and Biswas, C. 1989. Monoclonal antibody preparation and purification of a tumor cell collagenasestimulatory factor. *Cancer Res.* 49:3385.
- 9 Muracka, K., Nabeshima, K., Murayama, T., Biswas, C. and Koono, M. 1993. Enhanced expression of a tumor-cell-derived collagenasestimulatory factor in urothelial carcinoma: its usefulness as a tumor marker for bladder cancers. *Int. J. Cancer* 55:19.
- 10 Polette, M., Gilles, C., Marchand, V. et al. 1997. Tumor collagenase stimulatory factor (TCSF) expression and localization in human lung and breast cancers. J. Histochem. Cytochem. 45:703.
- 11 Basset, P., Bellocq, J. P., Wolf, C. et al. 1990. A novel metalloproteinase gene specifically expressed in stromal cells of breast carcinomas. *Nature* 348:699.
- 12 Majmudar, G., Nelson, B. R., Jensen, T. C. and Johnson, T. M. 1994. Increased expression of matrix metalloproteinase-3 (stromelysin-1) in cultured fibroblasts and basal cell carcinomas of nevoid basal cell carcinoma syndrome. *Mol. Carcinog.* 11:29.
- 13 Kasinrerk, W., Tokrasinwit, N. and Phunpae, P. 1999. CD147 monoclonal antibodies induce homotypic cell aggregation of monocytic cell line U937 via LFA-1/ICAM-1 pathway. *Immunology* 96 184
- 14 Khunkeawla, P., Moonsom, S., Staffler, G., Kongtawelert, P. and Kasinrerk, W. 2001. Engagement of CD147 molecule-induced cell aggregation through the activation of protein kinases and reorganization of the cytoskeleton. *Immunobiology* 203:659.
- 15 Renno, T., Wilson, A., Dunkel, C. et al. 2002. A role for CD147 in thymic development. J. Immunol. 168:4946.
- 16 Igakura, T., Kadomatsu, K., Kaname, T. et al. 1998. A null mutation in basigin, an immunoglobulin superfamily member, indicates its important roles in peri-implantation development and spermatogenesis. Dev. Biol. 194:152.
- 17 Staffler, G., Szekeres, A., Schutz, G. J. et al. 2003. Selective inhibition of T cell activation via CD147 through novel modulation of lipid rafts. J. Immunol. 171:1707.
- 18 Sun, J. and Hemler, M. E. 2001. Regulation of MMP-1 and MMP-2 production through CD147/extracellular matrix metalloproteinase inducer interactions. *Cancer Res.* 61:2276.
- 19 Smith, G. P. 1985. Filamentous fusion phage: novel expression vectors that display cloned antigens on the virion surface. Science 228:1315
- 20 Scott, J. K. and Smith, G. P. 1990. Searching for peptide ligands with an epitope library. *Science* 249:386.
- 21 Tayapiwatana, C., Árooncharus, P. and Kasinrerk, W. 2003. Displaying and epitope mapping of CD147 on VCSM13 phages: influence of Escherichia coli strains. J. Immunol, Methods 281:177.
- 22 Bass, S., Greene, R. and Wells, J. A. 1990. Hormone phage: an enrichment method for variant proteins with altered binding properties. *Proteins* 8:309.
- 23 Intasai, N., Arooncharus, P., Kasinrerk, W. and Tayapiwatana, C. 2003. Construction of high-density display of CD147 ectodomain on VCSM13 phage via gpVIII. effects of temperature, IPTG, and helper phage infection-period. *Protein Expr. Purif.* 32:323.

- 24 Malik, Z., Rothmann, C., Cycowitz, T., Cycowitz, Z. J. and Cohen, A. M. 1998. Spectral morphometric characterization of B-CLL cells versus normal small lympnocytes. J. Histochem. Cytochem. 46:1113.
- 25 Zheng, T. S., Schlosser, S. F., Dao, T. et al. 1998. Caspase-3 controls both cytoplasmic and nuclear events associated with Fas-mediated apoptosis in vivo. Proc. Natl Acad. Sci. USA 95: 13618
- 26 Kluza, J., Lansiaux, A., Wattez, N., Mahieu, C., Osheroff, N. and Bailly, C. 2000. Apoptotic response of HL-60 human leukemia cells to the antitumor drug TAS-103. Cancer Res. 60:4077.
- 27 Aubry, J. P., Blaecke, A., Lecoanet-Henchoz, S. et al. 1999. Annexin V used for measuring apoptosis in the early events of cellular cytotoxicity. Cytometry 37:197.
- 28 Liu, J., Yagi, T., Sadamori, H. et al. 2003. Annexin V assay-proven anti-apoptotic effect of ascorbic acid 2-glucoside after cold ischemia/reperfusion injury in rat liver transplantation. Acta Med. Okayama 57:209.
- 29 Chang, L. C., Madsen, S. A., Toelboell, T., Weber, P. S. and Burton, J. L. 2004. Effects of glucocorticoids on Fas gene expression in bovine blood neutrophils. J. Endocrinol. 183:569.
- Susin, S. A., Lorenzo, H. K., Zamzami, N. et al. 1999. Molecular characterization of mitochondrial apoptosis-inducing factor. Nature 397:441.
- 31 Iannolo, G., Minenkova, O., Gonfioni, S., Castagnoli, L. and Cesareni, G. 1997. Construction, exploitation and evolution of a new peptide library displayed at high density by fusion to the major coat protein of filamentous phage. *Biol. Chem.* 378:517.
- 32 Petrenko, V. A., Smith, G. P., Gong, X. and Quinn, T. 1996. A library of organic landscapes on filamentous phage. *Protein Eng.* 9:797.
- 33 Berditchevski, F., Chang, S., Bodorova, J. and Hemler, M. E. 1997. Generation of monoclonal antibodies to integrin-associated proteins. Evidence that alpha3beta1 complexes with EMMPRIN/basigin/OX47/M6. J. Biol. Chem. 272:29174.
- Cho, J. Y., Fox, D. A., Horejsi, V. et al. 2001. The functional interactions between CD98, beta1-integrins, and CD147 in the induction of U937 homotypic aggregation. *Blood* 98:374.
 Brown, E., Hooper, L., Ho, T. and Gresham, H. 1990. Integrin-
- 35 Brown, E., Hooper, L., Ho, T. and Gresham, H. 1990. Integrinassociated protein: a 50-kD plasma membrane antigen physically and functionally associated with integrins. J. Cell Biol. 111:2785.
- 36 Lindberg, F. P., Gresham, H. D., Reinhold, M. I. and Brown, E. J. 1996. Integrin-associated protein immunoglobulin domain is necessary for efficient vitronectin bead binding. J. Cell Biol. 134:1313.
- 37 Pushkarsky, T., Zybarth, G., Dubrovsky, L. et al. 2001. CD147 facilitates HIV-1 infection by interacting with virus-associated cyclophilin A. Proc. Natl Acad. Sci. USA 98:6360.
- 38 Yurchenko, V., O'Connor, M., Dai, W. W. et al. 2001. CD147 is a signaling receptor for cyclophilin B. Biochem. Biophys. Res. Commun. 288:786.
- 39 Yurchenko, V., Zybarth, G., O'Connor, M. et al. 2002. Active site residues of cyclophilin A are crucial for its signaling activity via CD147. J. Biol. Chem. 277:22959.
- 40 Yurchenko, V., Pushkarsky, T., Li, J. H., Dai, W. W., Sherry, B. and Bukrinsky, M. 2005. Regulation of CD147 cell surface expression: involvement of the proline residue in the CD147 transmembrane domain. J. Biol. Chem. 280:17013.
- 41 Kirk, P., Wilson, M. C., Heddle, C., Brown, M. H., Barclay, A. N. and Halestrap, A. P. 2000. CD147 is tightly associated with lactate transporters MCT1 and MCT4 and facilitates their cell surface expression. *EMBO J.* 19:3896.
- 42 Wilson, M. C., Meredith, D. and Halestrap, A. P. 2002. Fluorescence resonance energy transfer studies on the interaction between the factate transporter MCT1 and CD147 provide information on the topology and stoichiometry of the complex in situ. J. Biol. Chem. 277:3666.
- 43 Yoshida, S., Shibata, M., Yamamoto, S. et al. 2000. Homo-oligomer formation by basigin, an immunoglobulin superfamily member, via its N-terminal immunoglobulin domain. Eur. J. Biochem. 267, 4372.
- 44 Filavacek, W. S., Perelson, A. S., Sulzer, B. et al. 1999. Quantifying aggregation of IgE-FcepsilonRI by multivalent antigen. Biophys. J. 76 2421

- 45 Dintzis, H. M., Dintzis, R. Z. and Vogelstein, B. 1976. Molecular determinants of immunogenicity: the immunon model of immune response. Proc. Natl Acad. Sci. USA 73:3671.
- 46 Dintzis, R. Z., Middleton, M. H. and Dintzis, H. M. 1983. Studies on the immunogenicity and tolerogenicity of T-independent antigens. J. Immunol. 131.2196.
- 47 Sloan-Lancaster, J., Shaw, A. S., Rothbard, J. B. and Allen, P. M. 1994. Partial T cell signaling: altered phospho-zeta and lack of zap70 recruitment in APL-induced T cell anergy. Cell
- 48 Kersh, E. N., Shaw, A. S. and Allen, P. M. 1998. Fidelity of Ticell activation through multistep T cell receptor zeta phosphorylation. Science 281.572.
- 49 Konopleva, M., Tsao, T., Estrov, Z. et al. 2004. The synthetic triterpenoid 2-cyano-3,12-dioxooleana-1,9-dien-28-oic acid induces caspase-dependent and -independent apoptosis in acute myelogenous leukemia. Cancer Res. 64:7927.
- Daniel, D., Opelz, G., Mulder, A., Kleist, C. and Susal, C. 2004. Pathway of apoptosis induced in Jurkat T lymphoblasts by anti-HLA class I antibodies, Hum. Immunol. 65:189.
- Vande Velde, C., Cizeau, J., Dubik, D. et al. 2000. BNIP3 and genetic control of necrosis-like cell death through the mitochondrial permeability transition pore. Mol. Cell. Biol. 20:5454.
- 52 Cizeau, J., Ray, R., Chen, G., Gietz, R. D. and Greenberg, A. H. 2000. The C. elegans orthologue ceBNIP3 interacts with CED-9 and CED-3 but kills through a BH3- and caspase-independent mechanism. Oncogene 19:5453.

- 53 Sowter, H. M., Ratcliffe, P. J., Watson, P., Greenberg, A. H. and Harris, A. L. 2001. HIF-1-dependent regulation of hypoxic induction of the cell death factors BNIP3 and NIX in human tumors. Cancer Res. 61:6669.
- 54 Brown, M. H., Preston, S. and Barclay, A. N. 1995. A sensitive assay for detecting low-affinity interactions at the cell surface reveals no additional ligands for the adhesion pair rat CD2 and CD48. Eur. J. Immunol. 25:3222.
- 55 van der Merwe, P. A., Barclay, A. N., Mason, D. W. et al. 1994. Human cell-adhesion molecule CD2 binds CD58 (LFA-3) with a very low affinity and an extremely fast dissociation rate but does not bind CD48 or CD59. Biochemistry 33:10149.
- 56 Koch, C., Staffler, G., Huttinger, R. et al. 1999. T cell activationassociated epitopes of CD147 in regulation of the T cell response, and their definition by antibody affinity and antigen density. Int. Immunol, 11:777
- 57 Curtin, K. D., Meinertzhagen, I. A. and Wyman, R. J. 2005. Basigin (EMMPRIN/CD147) interacts with integrin to affect cellular architecture. J. Cell Sci. 118:2649.
- 58 Chiampanichayakul, S., Peng-In, P., Khunkaewla, P., Stockinger, H. and Kasinrerk, W. 2006. CD147 contains different bioactive epitopes involving the regulation of cell adhesion and lymphocyte activation. Immunobiology 211:167.
- Igakura, T., Kadomatsu, K., Taguchi, O. et al. 1996. Roles of basigin, a member of the immunoglobulin superfamily, in behavior as to an irritating odor, lymphocyte response, and blood-brain barrier. Biochem. Biophys. Res. Commun. 224:33.

A novel approach of using streptavidin magnetic bead sorting in vivo biotinylated survivin for monoclonal antibody production

Chatchai Tayapiwatana¹, Roongsiri Chotpadiwetkul², Watchara Kasinrerk^{1,3}*

¹Division of Clinical Immunology, Department of Medical Technology, Faculty of Associated Medical Sciences, Chiang Mai University, Chiang Mai 50200, Thailand.

²Division of Clinical Chemistry, Department of Medical Technology, Faculty of Associated Medical Sciences, Chiang Mai University, Chiang Mai 50200, Thailand.

³Medical Biotechnology Unit, National Center for Genetic Engineering and Biotechnology, National Science and Technology Development Agency at the Faculty of Associated Medical Sciences, Chiang Mai University, Chiang Mai 50200, Thailand.

*Corresponding author: Dr. Watchara Kasinrerk, Division of Clinical Immunology, Department of Medical Technology, Faculty of Associated Medical Sciences, Chiang Mai University, Chiang Mai 50200, Thailand. Tel.: +6653 945070; Fax: +6653 946043, E-mail: watchara@chiangmai.ac.th

Running title: A novel approach for monoclonal antibody production

Abbreviations: BCCP, biotin carboxyl carrier protein; ELISA, enzyme linked immunosorbent assay; SDS-PAGE, sodium dodecyl sulfate polyacrylamide gel electrophoresis; PCR, polymerase chain reaction; SVV, survivin

Abstract

One major obstacle in antibody production is the deficiency of highly purified immunogen. In this study, we described an alternative strategy for circumventing this problem. A nucleotide sequence encoding the full length of survivin was cloned into pAK400cb. After transforming into an *E. coli* Origami B strain, survivin-biotin carboxyl carrier protein (BCCP) fusion protein was generated in the cytoplasm, where the BCCP domain serves as a target for *in vivo* biotinylation. The biotinylated heterologous protein was subsequently immobilized on streptavidin coated magnetic particles and separated from other proteins in a magnetic field. The survivin coated beads were used to raise immune responses in BALB/c mice for hybridoma production. A number of hybrid clones were proved secreting anti-survivin antibodies. Three established clones were selected for single cell cloning. All generated monoclonal antibodies specifically reacted with the standard human recombinant survivin. Two out of three monoclonal antibodies recognized survivin in tumor extracts. The present method has advantages in facilitating monoclonal antibody production in that it makes antigen purification steps unnecessary.

Keywords: biotin carboxyl carrier protein, *in vivo* biotinylation, survivin, monoclonal antibody, hybridoma technique, *E. coli* Origami B strain

1. Introduction

5

The specificity of an antibody is generally a prerequisite for detection and discrimination of target substances by means of immunological assay. Since the establishment of the hybridoma technique (Kohler and Milstein, 1975), a large number of monoclonal antibodies (mAbs) have been produced for various purposes, including diagnostic, therapeutic and structural and functional studies of specific antigens. However, the currently available mAbs may not be sufficient for the vast requirements in the proteomic era. One major hurdle is the lack of highly purified immunogen, which limits the opportunity to acquire the candidate or unique mAbs. The availability of recombinant DNA technology makes it possible to clone any gene fragment and express the target protein (Makrides, 1996). The recombinant protein can normally be purified to near homogeneity from the crude protein mixture using affinity chromatography by employing fusion protein tags, i.e., glutathione-S transferase (Smith and Johnson, 1988), 6-histidine (Hochuli et al., 1987), or maltose binding protein (Di Guan et al., 1988).

Recently, Santala *et al.* reported the use of biotin carboxyl carrier protein (BCCP) as a fusion partner of single chain Fv (Santala and Lamminmaki, 2004). The heterologous hybrid molecule was biotinylated at the BCCP motif in *E. coli* Origami B strain (Prinz et al., 1997). Upon high oxidizing condition in the cytoplasmic space, both disulfide bonding and biotin conjugation occurred simultaneously. The advantage of a protein being tagged and made its natural conformation expanded the application in preparing the immunogen without traditional purification steps. We propose here a strategy of using the streptavidin coated magnetic particles for immobilizing and separating the biotinylated target-fusion molecules from the crude bacterial extracts. The protein coated beads serve as particulate antigens that are strongly immunogenic

for induction of immune responses. Hybridoma producing steps can be followed after immunizing mice with antigen coated magnetic beads.

Survivin, a member of inhibitor of apoptosis protein (IAP) family, was selected as a target for monoclonal antibody production. Survivin plays a dual role in both suppression of cell death and regulation of cell division ((Li et al., 1998; Li et al., 1999). The overexpression of survivin in various malignancies, but not in the adjacent normal tissues (Ambrosini et al., 1997), makes it an attractive target for cancer diagnosis and treatment. Unfavorable clinicopathological features, poor prognosis, disease progression, low survival and high recurrence rate, as well as therapeutic resistance, were associated with survivin expression (Adida et al., 1998; Swana et al., 1999; Adida et al., 2000; Islam et al., 2000; Kato, Kuwabara et al. 2001). Detection of survivin protein may serve as a molecular marker to diagnose cancer patients, identify individuals at risk of recurrence, and introduce proper treatment (Altieri, 2003). According to our approach, three mAbs against survivin were successfully generated and characterized. The method of using biotinylated fusion protein captured on streptavidin magnetic beads as an immunogen is rapid and does not require the purification of recombinant antigen.

2. Materials and methods

Construction of plasmid encoding survivin-BCCP (SVV-BCCP)

Human survivin encoding sequence was amplified from pcDNA3-human survivin (kindly provided by Professor Dario C. Altieri, Department of Cancer biology, University of Massachusetts Medical School, USA) using forward primer SVVNde I (5' GAGGAGGAGGTCATATGGGTGC CCCGACGTTGCCC 3') and reverse primer SVVEcoR I (5' GAGGAGGAGCTGAATTCATCCATGGCAGC CAGCTG 3') in 100 µl of a PCR mixture containing 5U ProofStart DNA polymerase (Qiagen, Hilden, Germany). The PCR cycling condition was started at one cycle at 95 °C for 5 min, followed by 34 cycles at 94 °C for 50 seconds, 50 °C for 50 seconds, and 72 °C for 1 minute. After 35 amplification cycles, the mixture was incubated at 72 °C for 10 min. The resulting PCR product was subsequently treated with Nde I (Fermentas, Vilnius, Lithuania) and EcoR I (Fermentas) at 37 °C for 18 h and purified using QI Aquick PCR purification kit (Qiagen). The pAK400cb vector, kindly provided Dr. Ville Santala (University of Turku, Finland) was treated with the same restriction enzymes and ligated with digested survivin-encoded sequence using T4 ligase enzyme (Roche Molecular Biochemicals, Indianapolis, IN). The resulting vector was named pAK400cb-SVV. For plasmid amplification, the pAK400cb-SVV was transformed into E. coli XL-1 Blue, which was then selected on LB agar containing 50 μg/ml chloramphenicol. The chloramphenicol-resistant colonies were selected and cultured in LB broth containing 50 µg/ml chloramphenicol for plasmid minipreparation. The inserted gene in the purified plasmid was verified by restriction fragment analysis with Nde I and EcoR I, and reamplification by PCR. After the correct clones were selected, the plasmids were purified and transformed into E. coli Origami B (Novagen, Madison, WI, USA) for protein expression.

Expression of biotinylated SVV-BCCP protein

E. coli Origami B harboring pAK400cb-SVV was cultured in 30 ml SB medium (30 g/l tryptone, 15 g/l yeast extract, and 10 g/l MOPS, pH 7.0) supplemented with glucose (0.05%), tetracycline (10 μg/ml), chloramphenicol (25 μg/ml), kanamycin (15 μg/ml), isopropyl-h-D-thiogalactopyranoside (IPTG, 100 μM), and 4 mM d-biotin (Sigma, St. Louis, MO). The cultures were incubated at 25 °C, 180 rpm for 22 hours. Bacteria were harvested by centrifugation at 4000 g, 4 °C for 10 min, resuspended in B-PER II extracting reagent (Pierce, Rockford, USA) and dialyzed against 25% ammonium buffer pH 9. The bacterial extract containing biotinylated SVV-BCCP was further lyophilized and kept at -70 °C.

Detection of biotinylated SVV-BCCP protein by ELISA

Microtiter plate (NUNC, Roskilde, Denmark) was coated with 0.5 μg of egg white avidin (Sigma) in 50 μl of carbonate/bicarbonate buffer, pH 9.6 at 4 °C for 18 hours. The coated wells were blocked with 2% skim milk in PBS for 1 hour at room temperature. After being washed three times with washing buffer (0.05% Tween 20 in PBS pH 7.2), 5 μg of lyophilized bacterial extract from pAK400cb-SVV transformed Origami B in 50 μl of 2% skim milk in PBS was added into each avidin coated well. After incubation at room temperature for 1 hour, the plate was washed three times with washing buffer. The bound SVV-BCCP was traced by adding 50 μl of 10 μg/ml mouse monoclonal anti-survivin (clone D-8) (Santa Cruz Biotechnology, California, USA). Subsequently, HRP conjugated rabbit-anti-mouse immunoglobulin antibody (DAKO, Hamburg, Germany) was added. After 1 hour incubation and washing, TMB color substrate was applied to each well. The plate was incubated at room temperature for 15

min for color development. The reaction was stopped by adding 1N HCl and the O.D. measured at 450 nm.

SDS-PAGE and Western immunoblotting

Bacterial extract containing SVV-BCCP or tumor tissue extract or recombinant human survivin (R&D system, Minneapolis, USA) was separated by SDS-PAGE under reducing conditions on a 12% polyacrylamide gel. The separated proteins were electroblotted onto PVDF membrane. The membrane was blocked at 4°C for 18 hours in 5% skim milk in PBS, pH 7.2, and then incubated with mouse anti-survivin mAbs and followed by HRP conjugated rabbit anti-mouse immunoglobulin antibodies (Dako) for 1 hour at room temperature on a shaking platform. After washing four times with 0.05% Tween 20 in PBS, pH 7.2, the immunoreactive bands were visualized by a chemiluminescent detection system (Pierce).

Separation of biotinylated SVV-BCCP by streptavidin-coated magnetic beads

Biotinylated SVV-BCCP was separated from crude bacterial extract using streptavidin-coated magnetic beads (MagnaBindTM Streptavidin Bead, Pierce). 200 μg of bacterial extract were mixed with 5x10⁷ washed streptavidin beads and incubated with gentle agitation for 30 minutes at room temperature. Reacted beads were subsequently trapped under a magnetic field and washed three times. Finally, beads were determined for the presence of fusion proteins by immunofluorescence and flow cytometry.

Detection of survivin coated magnetic beads by flow cytometry

SVV-BCCP 2.5x10⁶ beads were incubated with 5 µg/ml mouse anti-survivin mAb (Santa Cruz Biotechnology) in 50 µl total volume at room temperature for 30 min

with gentle agitation. After three-time washing, FITC conjugated sheep anti-mouse immunoglobulins antibody (Chemicon International, Melbourne, Australia) was added and incubated with gentle agitation for 30 min at room temperature. The beads were then washed three times and resuspended with 400 µl of 1% paraformaldehyde in PBS. The fixed beads were further analyzed using a flow cytometer (FACSCalibur, Becton Dickinson, Sunnyvale, USA).

Immunization schedule

Two female Balb/c mice were intraperitoneally immunized with 5×10^7 magnetic beads coated with SVV-BCCP in 500 μ l PBS three times at two-week intervals. Blood samples were collected from the immunized mice by tail bleeding prior to each antigen injection. Sera were separated and stored at -20°C.

Analysis of anti-survivin antibodies in mice sera by ELISA

The kinetics of anti-survivin polyclonal antibodies induced by SVV-BCCP bead immunization were determined using indirect ELISA. Microtiter plate (NUNC) was coated with 0.5 µg avidin for overnight at 4°C. The coated plate was blocked with 2% skim milk in PBS, and then 5 µg of bacterial extract containing SVV-BCCP was added into the avidin coated wells. After washing three times, various dilutions of mice sera were added into the wells. Plate was incubated for 1 hour and washed 3 times. To trace the antibody binding, HRP conjugated rabbit anti-mouse immunoglobulin antibody (Dako) was added. After incubation and washing, TMB substrate was added. 1N HCl was used to stop the reaction and the colorimetric signal was measured at O.D. 450 nm.

Hybrido ma production

Spleen cells were collected from the immunized mouse and fused with P3-X63Ag8.653 myeloma cells by standard hybridoma technique using 50% polyethylene

glycol (Sigma). After HAT medium selection, culture supernatants from the hybrid containing wells were collected. The supernatants were then determined for antibody reactivity against survivin by indirect ELISA using SVV-BCCP and CD147-BCCP as antigens. The hybridomas showing positive reactivity with SVV-BCCP but negative with CD147-BCCP were selected and subcloned by limiting dilution. The isotype of monoclonal antibodies were determined by using the isotyping ELISA kit (Sigma).

Protein extraction from biopsy tissues

The fresh frozen tumor tissue (0.3 g) was homogenized in 69 mM SDS lysis buffer, in the presence of protease inhibitors (Roche, Basel, Switzerland) The tissue homogenate was incubated at 95°C for 10 min and centrifuged at 15,000 g at 4 °C for 15 min. The supernatant was collected and kept at -70°C until used.

Immunofluorescence analysis of survivin

For cell surface staining, cells were washed 3 times with PBS and adjusted to $1X10^7$ cells/ml with PBS containing 1% bovine serum albumin (BSA) and 0.02% sodium azide (1% BSA-PBS-NaN₃). To block the nonspecific Fc receptor- mediated binding of antibodies, cells were incubated for 30 min at 4 °C with 10% human AB serum before staining. Fifty microliters of blocked cells were then incubated with hybridoma culture supernatants or anti-survivin mAb for 30 min at 4 °C. After twice washing with 1%BSA-PBS-NaN₃, cells were incubated with FITC-conjugated sheep $F(ab')_2$ anti-mouse immunoglobulins (Chemicon International) for 30 min. Membrane fluorescence was analyzed using a flow cytometer (FACSCalibur, Becton Dickinson).

For intracellular staining, Fc receptor blocked cells were fixed with fixative medium (Caltag laboratories, Burlingame, USA) for 15 min, and permeabilized using

permeabilization medium (Caltag laboratories). The permeabilized cells were then incubated for 30 min with hybridoma culture supernatants. Then, FITC-conjugated sheep anti-mouse immunoglobulin antibody (Chemicon International) was added and incubated for 30 min. After twice washing, cells were fixed in 1% paraformaldehyde-PBS and analyzed using a flow cytometer.

3. Results

Construction of plasmid containing the survivin gene

In order to produce recombinant SVV-BCCP, the plasmid pAK400cb-SVV was constructed. Primer sets were designed such that *Nde* I and *EcoR* I restriction sites were incorporated into the ends of the survivin coding sequences amplified from the pcDNA3-human survivin. The PCR product was visualized at approximately 450 bp (data not shown). The amplified product was further purified, then cleaved with *Nde* I and *EcoR* I and subcloned into pAK400cb in the correct reading frame. The recombinant plasmid was subsequently transformed into *E. coli* XL-1 Blue. Several colonies from chloramphenical plates were selected for plasmid extraction and screened by PCR and restriction analysis. The recombinant clones harboring the correct amplified product and cleaved insert of human survivin at 450 bp were chosen for subsequent protein expression. The generated recombinant plasmid was named pAK400cb-SVV.

SVV-BCCP produced from E. coli Origami B

Heterologous SVV-BCCP was synthesized in the cytoplasm of pAK400cb-SVV transformed *E. coli* Origami B. *In vivo* biotinylation at BCCP occurred along with enhanced expression of recombinant protein when culturing in biotin and IPTG-containing medium. The bacterial cell lysate was analyzed for SVV-BCCP by avidin capture ELISA. Wells coated with avidin followed by crude extract from pAK400cb-SVV transformed *E. coli* demonstrated positive signal when traced with anti-survivin mAb, clone D-8 (Asanuma et al., 2004) (Table 1). In contrast, the signal was low when crude extract from *E. coli* transformed pAK400cb-CD147 (irrelevant protein) was substituted for pAK400cb-SVV. These data confirmed that survivin was produced in

transformed *E. coli*. In addition, the data verified that survivin was produced as a fusion protein with BCCP.

The molecular size of the recombinant product was examined by Western immunoblotting using anti-survivin mAb. The reactive bands at approximately 30-35 kDa and suspected degraded products at approximately 15 kDa were visualized (Fig. 1).

Coating of SVV-BCCP on streptavidin beads

To prepare survivin coated beads for use as a particulate immunogen, the produced SVV-BCCP were incubated with streptavidin-coated magnetic beads. The coated beads were detected by anti-survivin antibody, clone D-8. All coated beads gave a positive FITC signal as observed by flow cytometry (Fig. 2). This suggested the anchoring of biotinylated SVV-BCCP on the magnetic particles. The complex was further sorted under the magnetic field for using as an immunogen.

Induction of anti-survivin polyclonal antibodies by SVV-BCCP beads imunization

SVV-BCCP beads were injected into two BALB/c mice at bi-weekly intervals. Antibodies generated in the immunized mice were determined by indirect ELISA using SVV-BCCP fusion protein as antigens. Antibodies could be detected after the 2nd immunization and slightly increased after the 3rd immunization (Fig. 3). Serum titer after the 3rd antigen immunization was more than 1:320,000 (data not shown). The results demonstrated that the immunogen-captured beads could be used to induce the antibody response.

Establishment of hybridoma secreting anti-survivin mAbs

Cell fusion was performed using mouse spleen cells immunized with magnetic bead-sorted SVV-BCCP. A total of 368 hybridoma clones resulted from 960 plated

wells. Nine of them secreted antibodies which reacted with SVV-BCCP in ELISA but did not react with an irrelevant recombinant protein, CD147-BCCP. These results indicated that the reactive epitopes for these hybridoma clones were located on the survivin portion. Consequently, three hybridomas secreting anti-survivin antibodies were selected and re-cloned by limiting dilution. All generated single hybrid clones were reconfirmed for their antibody activity by ELISA (Fig. 4). These generated clones were named MT-SVV1, MT-SVV2 and MT-SVV3. The isotype of all clones was identified as IgG1

Western immunoblotting of anti-survivin mAbs

To test the specificity of the three established anti-survivin mAbs, immunoblotting was performed using bacterial cell lysate containing SVV-BCCP. As shown in Fig 5, the immunoblotting patterns obtained from MT-SVV1, MT-SVV2 and MT-SVV3 mAbs and commercial anti-survivin mAb clone D-8 were similar. All mAbs reacted to a protein band at approximately 30-35 kDa, which was the recombinant SVV-BCCP (lane 1A-3A and 6A). None of these mAbs recognize the irrelevant target, CD147-BCCP (Fig. 5B). In contrast, when CD147 mAb clone M6-1D4 (Kasinrerk et al., 1999) was used as a detector, no reactive band appeared in lanes loaded with bacterial lysate containing SVV-BCCP (Fig. 5A, lane 4). The positive bands appeared only in lane containing CD147-BCCP (Fig. 5B, lane 6). To confirm the specificity of the generated mAbs, recombinant human survivin purchased from R&D system (Minneapolis, MN, USA) was applied as a control. MT-SVV1, MT-SVV2, MT-SVV3 as well as anti-survivin mAb clone D-8 reacted with a protein band of approximately 16 kDa (Fig. 6).

The generated mAbs were also used to detect survivin extracted from tumor tissue. The mAbs MT-SVV1, MT-SVV3, but not MT-SVV2, and anti-survivin mAb

90

clone D-8 reacted with survivin protein, molecular weight of 16 kDa, contained in the tissue lysate. All mAbs, including control anti-survivin mAb clone D-8, showed an extra band at the molecular weight of 55 kDa (Fig. 7).

Intracellular survivin detection by flow cytometry

Intracellular survivin expression in a leukemic cell line U937 was determined using the generated mAbs. As shown in Fig. 8, all generated mAb showed positive reactivity by intracellular staining. None of mAbs bound to any proteins expressed on the cell surface.

4. Discussion

5

Several fusion tags are generally employed for recombinant protein detection and purification. In particular cases, the purified product is further used for antibody production. The inherit characters of tags determine the rate of success in specific applications. Some tags, for example HIS (Tucker and Grisshammer, 1996), have an advantage in small size; but the specificity for detection or purification purpose is rather low causing high detection background and contamination by irrelevant proteins. In the case of maltose-binding protein tag (Kapust and Waugh, 1999), it promotes the solubility of the recombinant protein by suppressing inclusion body formation. This feature benefits production of heterologous protein in E. coli. However, the molecular size of maltose-binding protein is high; thus it consumes the substrate for protein production and may interfere with the function of recombinant protein. The GST tag also has a bulky size, and tends to form dimers (Waugh, 2005). In addition, the recombinant protein containing the GST tag is not suitable for preparing an immunogen, since the tag itself is strongly immunogenic. The possibility of obtaining specific antibodies to the target portion is, therefore, reduced. Recently, Santala et al. described an alternative fusion tag, i.e., biotin carboxyl carrier protein (BCCP). Biotin carboxyl carrier protein (BCCP) is the small biotinylated subunit of E. coli acetyl-CoA carboxylase (ACC) (Chapman-Smith and Cronan, 1999). The biotinyl domain was fused to an antibody fragment, ScFv, for immunoassay development. A similar concept was applied to generate a protein with AviTag, a biotinyl domain containing 15 amino acids. The target was immobilized on streptavidin-coated magnetic beads for phagedisplay selection experiments (Scholle et al., 2004).

In this study, the BCCP fusion tag was cloned in frame and downstream to the human survivin encoding sequence. The SVV-BCCP fusion protein was expressed in E.

coli Origami B after culturing at 25°C with IPTG induction. The biotinylation of the recombinant molecule obtained in bacterial crude extract was verified using ELISA. A specific anti-survivin mAb clone D-8 (Asanuma et al., 2004) recognized the fusion protein captured on plate coated with egg white avidin. The reaction bridge confirmed the presence of SVV-BCCP fusion protein in the transformed bacterial lysate. In contrast, there was no survivin captured on the wells coated with crude extract from mock transformed Origami B. This result excluded non-specific binding of antisurvivin mAb clone D-8 to the irrelevant proteins. In addition, the heterologous molecule was detected in Western immunoblotting by specific anti-survivin mAb. CD147 mAb showed negative binding to SVV-BCCP target and assured the specificity of assays. The expressed survivin in high oxidizing conditions of the Origami B cytoplasm promoted the correct folding, which was determined by the accomplishment of in vivo biotinylation in BCCP portion (Chapman-Smith and Cronan, 1999). Since the protein was biotinylated outside the survivin segment, the overall conformation and native epitopes were preserved. In comparison with chemically performed biotinylation, the antigenicity of the target molecule may be altered upon conjugation.

The purification process is known to be the most cumbersome step after obtaining the recombinant protein. Normally, affinity chromatography using a column conjugated with a specific target for capturing the fusion tag domain is required. The purification yield is usually low, especially when the concentration of heterologous protein is low. To overcome these problems, in this study, streptavidin coated magnetic beads were used to sort the SVV-BCCP from bacterial crude extract. The magnetic field was applied to trap and separate the beads from the solution mixture. The fusion heterologous molecule linked to the bead surface was proven by flow cytometry. In an attempt to produce monoclonal antibody to suvivin, the survivin fusion protein coated

beads were used as an immunogen. Regarding single biotinylation motive proximity to the C-terminal, BCCP formed the stalk for protruding survivin from the bead surface. This allowed B-lymphocytes to respond to survivin epitopes more efficiently. In addition, the immunogen was prepared in particulate form, which enhanced the immune response in contrast to the soluble form. Hyperimmune serum from immunized mouse showed potent antibody response, which was adequate for conventional hybridoma technique.

To screen the hybridoma producing anti-survivin antibodies, SVV-BCCP and CD147-BCCP captured on plates using egg white avidin were used as an antigen. By this screening system, hybridomas secreting anti-streptavidin antibodies were excluded, since the egg avidin was used in the ELISA assay whereas streptavidin was used for capturing SVV-BCCP on beads in the immunization step. Three hybrid clones, MT-SVV1, MT-SVV2 and MT-SVV3, were established in this study. All secreted antibodies directed against survivin antigenic determinants and did not react with BCCP. Some other hybrid clones produced antibodies which reacted with both SVV-BCCP and CD147-BCCP and were assumed to engage the BCCP epitopes (data not shown). In the Western immunoblotting experiment, all generated anti-SVV mAbs showed a similar pattern to anti-survivin mAb clone D-8 when recombinant SVV-BCCP or standard human recombinant survivin was used as an antigen. The determinants recognized by all mAbs are presumably linear, since reducing conditions and heat denaturation were introduced in SDS-PAGE. However, only the survivin mAb clone D8, MT-SVV1 and MT-SVV3 showed a positive result with survivin at 16 kDa from the tumor extract. We have no experimental results that bear on the question of why mAb MT-SVV2 fails to bind to survivin in tumor extract. It is possible that mAb MT-SVV2 binds to a particular epitope, which is destroyed during tissue extraction.

50

In leukemic cells, all generated survivin mAbs bound to the intracellular survivin expressed in U937. As predicted, these mAbs did not react with any proteins expressed on the cell surface. These results indicated that the generated anti-SVV mAbs may have a high potential for applying in the immunohistochemistry technique.

In this study, an alternative strategy of immunogen preparation for mAb production was demonstrated. The technique overcomes the lack of purified antigen problem. In addition, the specific domain of the target molecule could be selectively cloned and expressed with *in vivo* biotinylation. Further step in a cumbersome purification processes are, thus, eliminated and substituted by a single antigen capturing step. Streptavidin coated magnetic beads specifically interact with the recombinant protein containing the BCCP domain, which is biotinylated. The protein captured beads can be directly used as particulate antigen for induction of antibody production. The success in production of mAbs against survivin should be applicable to other target proteins for which gene coding sequences are known.

Acknowledgments

This work was supported by The National Center for Genetic Engineering and Biotechnology (BIOTEC) of the National Science and Technology Development Agency, Thailand and the Thailand Research Fund. We are thankful to Nitwara Wikan, Surasit Bupachat and Anuson Lekawipat for expert technical assistance and Dr. Dale Taneyhill for proofreading of the manuscript.

References

- Adida, C., Berrebi, D., Peuchmaur, M., Reyes-Mugica, M. and Altieri, D.C. (1998)

 Anti-apoptosis gene, survivin, and prognosis of neuroblastoma. Lancet 351,

 882.
- Adida, C., Recher, C., Raffoux, E., Daniel, M.T., Taksin, A.L., Rousselot, P., Sigaux, F., Degos, L., Altieri, D.C. and Dombret, H. (2000b) Expression and prognostic significance of survivin in de novo acute myeloid leukaemia. Br. J. Haematol. 111, 196.
- Altieri, D.C. (2003) Survivin in apoptosis control and cell cycle regulation in cancer.

 Prog. Cell Cycle Res. 5, 447.
- Ambrosini, G., Adida, C. and Altieri, D.C. (1997) A novel anti-apoptosis gene, survivin, expressed in cancer and lymphoma. Nat. Med. 3, 917.
- Asanuma, K., et al. 2004. Survivin enhances Fas ligand expression via up-regulation of specificity protein 1-mediated gene transcription in colon cancer cells. J. Immunol. 172, 3922.
- Chapman-Smith, A., Cronan, J.E. 1999. The enzymatic biotinylation of proteins: a post-translational modification of exceptional specificity. Trends Biochem. Sci. 24, 359.
- Di Guan, C., Li, P., Riggs, P.D., Inouye, H. 1988. Vectors that facilitate the expression and purification of foreign peptides in *Escherichia coli* by fusion to maltosebinding protein. Gene 15, 21.
- Hochuli, E., Dobeli, H., Schacher, A. 1987. New metal chelate adsorbent selective for proteins and peptides containing neighbouring histidine residues. J. Chromatogr. 18, 177.

- Islam, A., Kageyama, H., Takada, N., Kawamoto, T., Takayasu, H., Isogai, E., Ohira, M., Hashizume, K., Kobayashi, H., Kaneko, Y. and Nakagawara, A. (2000)

 High expression of Survivin, mapped to 17q25, is significantly associated with poor prognostic factors and promotes cell survival in human neuroblastoma.

 Oncogene 19, 617.
- Kapust, R.B., Waugh, D.S. 1999. *Escherichia coli* maltose-binding protein is uncommonly effective at promoting the solubility of polypeptides to which it is fused. Protein Sci. 8, 1668.
- Kasinrerk, W., Tokrasinwit, N., Phunpae, P. 1999. CD147 monoclonal antibodies induce homotypic cell aggregation of monocytic cell line U937 via LFA-1/ICAM-1 pathway. Immunology 96, 184.
- Kato, J., Kuwabara, Y., Mitani, M., Shinoda, N., Sato, A., Toyama, T., Mitsui, A., Nishiwaki, T., Moriyama, S., Kudo, J. and Fujii, Y. (2001) Expression of survivin in esophageal cancer: correlation with the prognosis and response to chemotherapy. Int. J. Cancer 95, 92.
- Kohler, G., Milstein, C., 1975. Continuous cultures of fused cells secreting antibody of predefined specificity. Nature 256, 495.
- Li, F., Ackermann, E.J., Bennett, C.F., Rothermel, A.L., Plescia, J., Tognin, S., Villa, A., Marchisio, P.C. and Altieri, D.C. (1999) Pleiotropic cell-division defects and apoptosis induced by interference with survivin function. Nat. Cell Biol. 1, 461.
- Li, F., Ambrosini, G., Chu, E.Y., Plescia, J., Tognin, S., Marchisio, P.C. and Altieri, D.C. (1998) Control of apoptosis and mitotic spindle checkpoint by survivin. Nature 396, 580.

- Makrides, S.C., 1996. Strategies for achieving high-level expression of genes in Escherichia coli. Microbiol. Rev. 60, 512.
- Prinz, W.A., Aslund, F., Holmgren, A., Beckwith, J. 1997. The role of the thioredoxin and glutaredoxin pathways in reducing protein disulfide bonds in the Escherichia coli cytoplasm. J. Biol. Chem. 272, 15661.
- Santala, V., Lamminmaki, U. 2004. Production of a biotinylated single-chain antibody fragment in the cytoplasm of *Escherichia coli*. J. Immunol. Methods 284, 165.
- Scholle, M.D., Collart, F.R., Kay, B.K. 2004. *In vivo* biotinylated proteins as targets for phage-display selection experiments. Protein Expr. Purif. 37, 243.
- Smith, D.B., Johnson, K.S., 1988. Single-step purification of polypeptides expressed in *Escherichia coli* as fusions with glutathione S-transferase. Gene 67, 31.
- Swana, H.S., Grossman, D., Anthony, J.N., Weiss, R.M. and Altieri, D.C. (1999)
 Tumor content of the antiapoptosis molecule survivin and recurrence of bladder cancer. N. Engl. J. Med. 341, 452.
- Tucker, J., Grisshammer, R. 1996. Purification of a rat neurotens in receptor expressed in *Escherichia coli*. Biochem. J. 317, 891.
- Waugh, D.S. 2005. Making the most of affinity tags. Trends Biotechnol. 23, 316.

Figure Legends

Figure 1. Western immunoblot analysis of SVV-BCCP produced by *E. coli* Origami B. pAK400cb-SVV (lane 1) and pAK400cb-CD147 transformed *E. coli* (lane 2) crude lysates were separated by SDS-PAGE under reducing conditions and blotted on a PVDF membrane. The membrane was incubated with anti-survivin mAb clone D-8. The reactive bands were visualized using chemiluminescent system. Protein markers with indicated molecular weight in kDa are shown.

Figure 2. Validation of SVV-BCCP bound on the streptavidin-coated magnetic beads by flow cytometry. Streptavidin-coated beads were incubated with SVV-BCCP and harvested under a magnetic field. The SVV-BCCP beads were probed with anti-survivin mAb clone D-8 (A) or with isotype matched control mAb, Thal N/B (B). Beads without SVV-BCCP were probed with anti-survivin mAb clone D-8 (C).

Figure 3. The kinetics of antibody responses in mice immunized with SVV-BCCP coated bead. Plate was coated with egg white avidin followed by crude bacterial extract containing SVV-BCCP. Mice sera at dilution 1:1,000 were applied to each well. Pre-immune sera (Pre-immune), sera obtained at 7 days after the first immunization (first serum), at 7 days after the second immunization (second serum) and at 7 days after the third immunization (third serum) are shown.

Figure 4. ELISA for verifying the specificity of mAbs MT-SVV1, MT-SVV2 and MT-SVV3. Plate was coated with egg white avidin followed by crude bacterial extract containing SVV-BCCP or SVV-CD147. Indicated mAbs were added to the ELISA plate. mAb D-8 is anti-survivin mAb purchased from Santa Cruz Biotechnology; M6-1B9 is an anti-CD147 mAb (Kasinrerk et al. 1999).

Figure 5. Western immunoblotting of mAbs MT-SVV1, MT-SVV2 and MT-SVV3. Crude extracts of pAK400cb-SVV (A) or pAK400cb-CD147 (B) transformed *E. coli* were separated by SDS-PAGE and blotted on PVDF membranes. In A, the membrane was incubated with MT-SVV1 (lane 1), MT-SVV2 (lane 2), MT-SVV3 (lane 3), anti-CD147 mAb M6-1D4 (lane 4), myeloma culture supernatant (lane 5), anti-survivin mAb clone D-8 (lane 6). In B, the membrane was incubated with MT-SVV1 (lane 1), MT-SVV2 (lane 2), MT-SVV3 (lane 3), anti-survivin mAb clone D-8 (lane 4), myeloma culture supernatant (lane 5), anti-CD147 mAb M6-1D4 (lane 6). Protein markers with molecular weight indicated in kDa are shown.

Figure 6. Reactivity of mAbs MT-SVV1, MT-SVV2 and MT-SVV3 against recombinant human survivin. Purified full-length recombinant human survivin was separated by SDS-PAGE under reducing condition and blotted onto a PVDF membrane. The membrane was reacted with MT-SVV1 (lane 1), MT-SVV2 (lane 2), MT-SVV3 (lane 3), anti-survivin mAb clone D-8 (lane 4) and anti-CD45 mAb MT45 (lane 5). Protein markers with indicated molecular weight in kDa are shown.

Figure 7. Reactivity of mAbs MT-SVV1, MT-SVV2 and MT-SVV3 with tumor tissue extract. Tumor tissue homogenate was separated by SDS-PAGE under reducing conditions and blotted onto a PVDF membrane. The membrane was reacted with MT-SVV1 (lane 1), MT-SVV2 (lane 2), MT-SVV3 (lane 3), iostyped matched control mAb Thal N/B (lane 4), myeloma culture supernatant (lane 5) and anti-survivin mAb clone D-8 (lane 6). Protein markers with indicated molecular weight in kDa are hown.

Figure 8. Immunofluorescence analysis of the reactivity of anti-survivin mAbs by intracellular (A) and surface staining (B) of U937 cells. Solid lines represent the

immunofluorescence profiles of cells stained with indicated mAbs and dashed lines represent background fluorescence of the conjugate control.

Table I. Determination of survivin-BCCP in *E. coli* crude extracts by avidin captured ELISA

Egg white avidin 1	E. coli extract ²	mAb ³	O.D.450 ⁴
+	pAK400cb-SVV	anti-survivin ^a	2.30
+	wild-type	anti-survivin	0.06
+	pAK400cb-SVV	-	0.06
+	wild-type	-	0.06
+	pAK400cb-CD147	anti-CD147 ^b	2.66
-	pAK400cb-SVV	anti-survivin	0.19

¹ Plate was coated with or without egg white avidin.

² E. coli Origami B strain was transformed with the indicated vector and crude extracts were tested for the presence of surivivin-BCCP by ELISA.

³ mAbs used: ^aanti-survivin mAb clone D-8 purchased from Santa Cruz Biotechnology; ^banti-CD147 mAb clone M6-2F9 (Kasinrerk et al. 1999).

⁴ mean of three independent experiments.

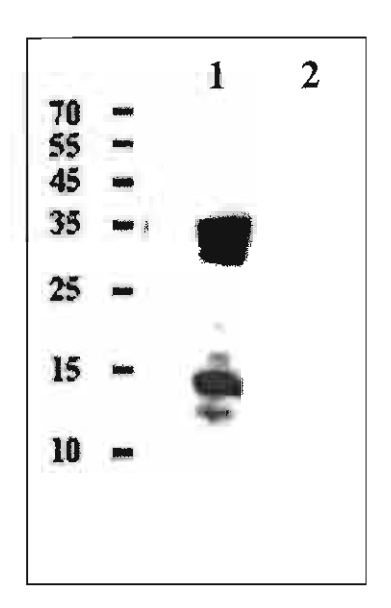


Figure 1.

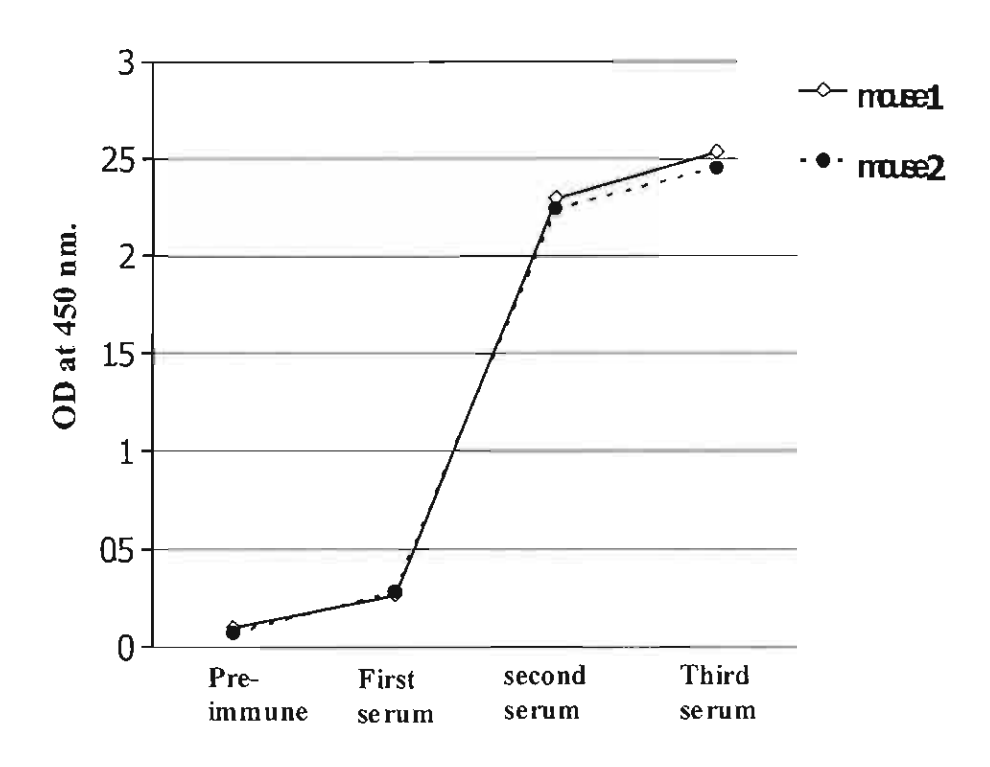


Figure 3.

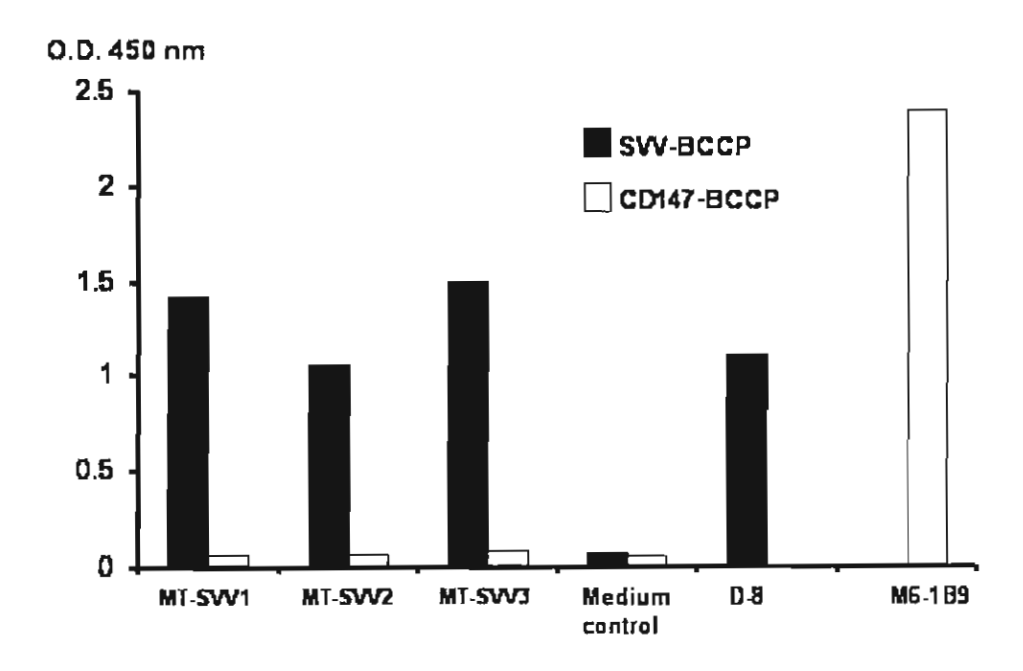


Figure 4.

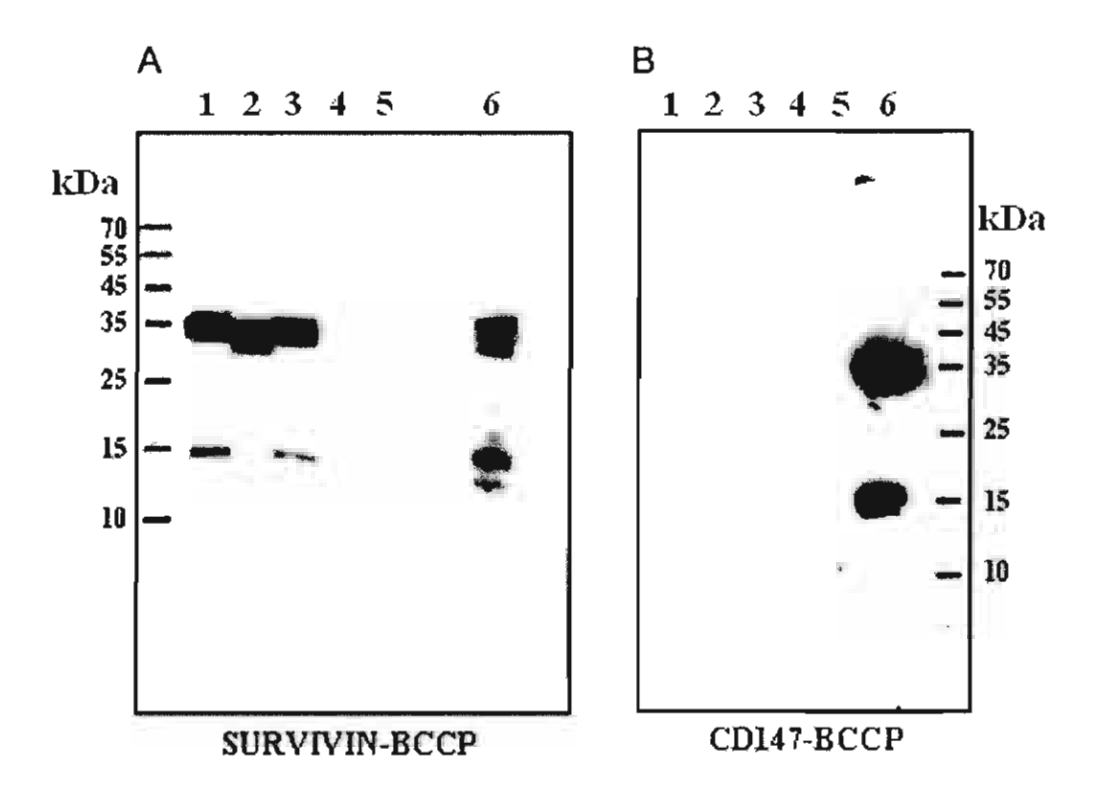


Figure 5.

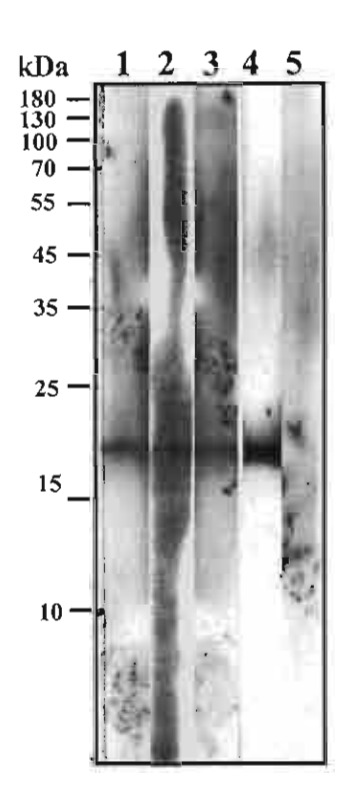


Figure 6.

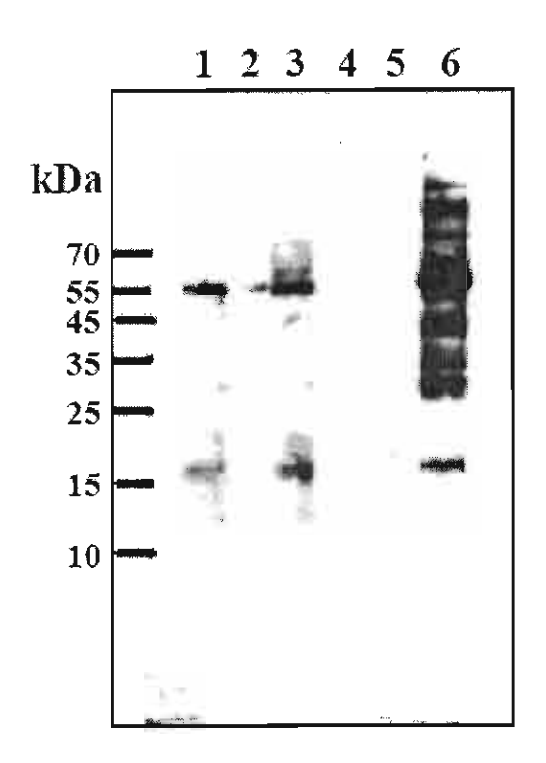


Figure 7.

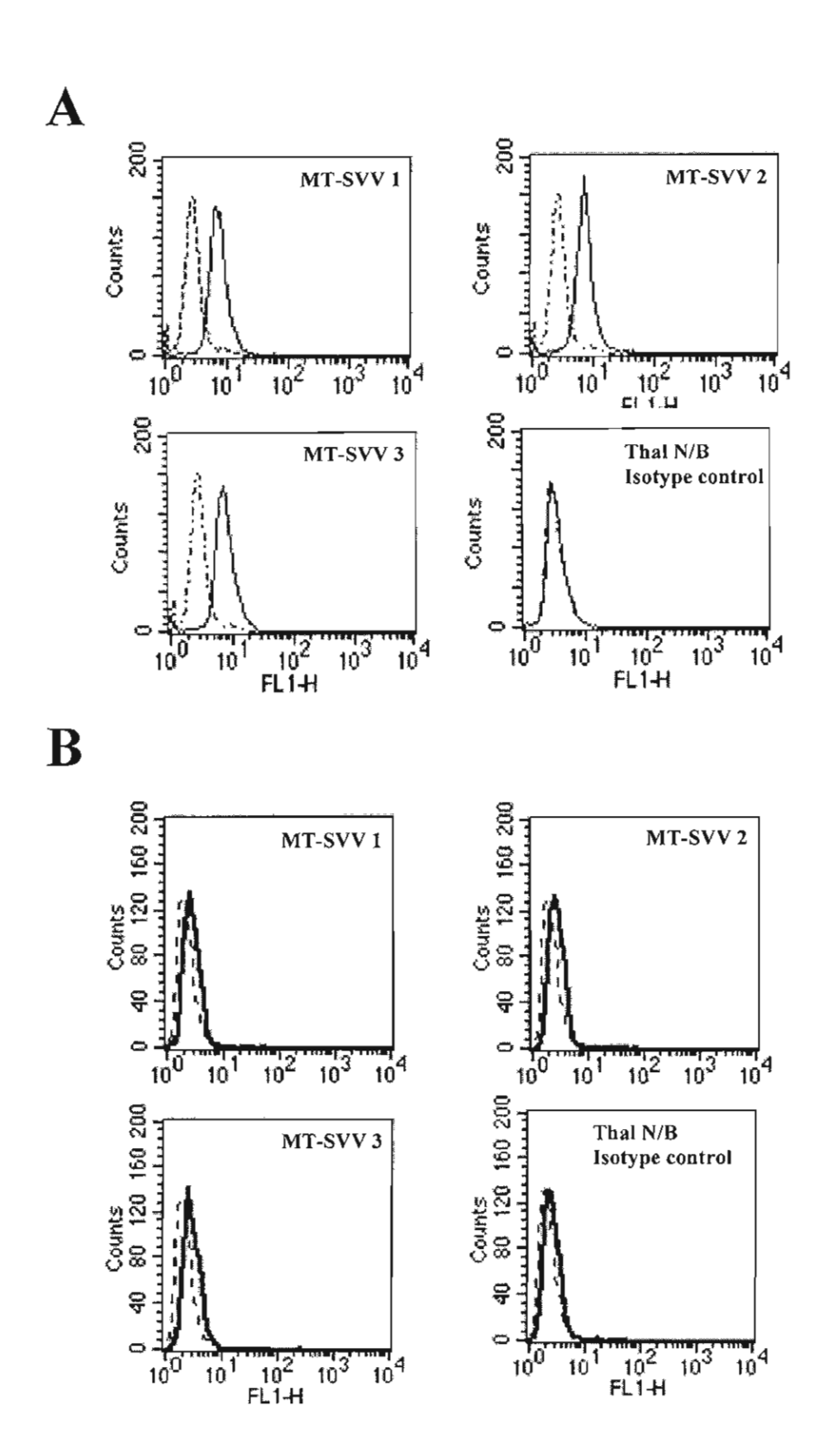


Figure 8.